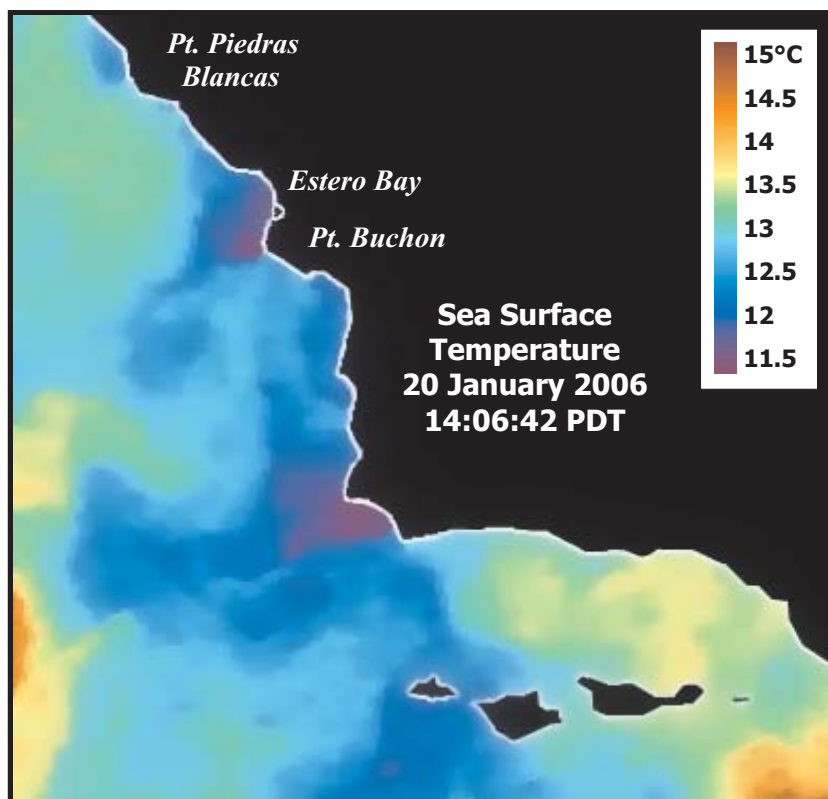


**City of Morro Bay and
Cayucos Sanitary District**

OFFSHORE MONITORING AND REPORTING PROGRAM

QUARTERLY REPORT

WATER-COLUMN SAMPLING JANUARY 2006 SURVEY



Marine Research Specialists

**3140 Telegraph Rd., Suite A
Ventura, California 93003**

Report to

**City of Morro Bay and
Cayucos Sanitary District**

**955 Shasta Avenue
Morro Bay, California 93442
(805) 772-6272**

**OFFSHORE MONITORING
AND
REPORTING PROGRAM**

QUARTERLY REPORT

**WATER-COLUMN SAMPLING
JANURAY 2006**

Prepared by

**Douglas A. Coats
and
Bonnie Luke**

Marine Research Specialists

**3140 Telegraph Rd., Suite A
Ventura, California 93003**

**Telephone: (805) 644-1180
Telefax: (805) 289-3935
E-mail: Doug.Coats@mrsenv.com**

March 2006

marine research specialists

3140 Telegraph Road, Suite A · Ventura, CA 93003 · (805) 644-1180

Mr. Bruce Keogh
Wastewater Division Manager
City of Morro Bay
955 Shasta Avenue
Morro Bay, CA 93442

9 March 2006

Reference: Quarterly Receiving-Water Report – January 2006

Dear Mr. Keogh:

Enclosed is the Quarterly Report for the Water-Quality Survey conducted on 17 January 2006. This first-quarter survey assessed the effectiveness of effluent dispersion during winter oceanographic conditions. Based on quantitative analyses of continuous instrumental measurements and qualitative visual observations, the wastewater discharge was found to be in compliance with the receiving-water limitations specified in the NPDES discharge permit, and with the objectives of the California Ocean Plan.

High-precision measurements clearly delineated very slight lateral perturbations in all six seawater properties. These measurements demonstrated that detectable wastewater constituents were confined to the zone of initial dilution where receiving-water limitations do not apply. Beyond that zone, small anomalies in temperature, turbidity, dissolved oxygen, and pH were generated by the upward displacement of ambient seawater, rather than the presence of wastewater constituents. All of the measurements were indicative of low contaminant concentrations within the discharged wastewater, and of an outfall operating as designed.

Please contact the undersigned if you have any questions regarding this report.

Sincerely,

Douglas A. Coats, Ph.D.
Program Manager

Enclosure (Seven Copies)

I certify under penalty of law that this document and all attachments were prepared under my direction or supervision in accordance with a system designed to assure that qualified personnel properly gather and evaluate the information submitted. Based on my inquiry of the person or persons who manage the system, or those persons directly responsible for gathering the information, the information submitted is, to the best of my knowledge and belief, true, accurate, and complete. I am aware that there are significant penalties for submitting false information, including the possibility of fine and imprisonment for knowing violations.

Mr. Bruce Ambo
City of Morro Bay

Date _____

TABLE OF CONTENTS

LIST OF FIGURES	i
LIST OF TABLES	ii
INTRODUCTION	1
STATION LOCATIONS	2
METHODS	9
<i>Ancillary Measurements</i>	9
<i>Instrumental Measurements</i>	10
<i>Temporal Trends in the pH Sensor</i>	12
RESULTS.....	12
<i>Beneficial Use</i>	13
<i>Ambient Seawater Properties</i>	13
<i>Lateral Variability</i>	14
<i>Discharge-Related Perturbations</i>	16
<i>Initial Dilution Computations</i>	18
DISCUSSION	20
<i>Outfall Performance</i>	20
<i>NPDES Permit Limits</i>	21
<i>Light Transmittance</i>	21
<i>Dissolved Oxygen</i>	22
<i>pH</i>	22
<i>Temperature and Salinity</i>	22
<i>Conclusions</i>	23
REFERENCES	24

APPENDICES

- A. Water-Quality Profiles and Vertical Sections
- B. Tables of Profile Data and Standard Observations

LIST OF FIGURES

Figure 1. Regional Setting of Receiving-Water Sampling Stations within Estero Bay	3
Figure 2. Offshore Water Sampling Locations on 17 January 2006	5
Figure 3. Estero Bay Tidal Level during the Field Survey of 17 January 2006.....	8

LIST OF TABLES

Table 1. Description of Receiving-Water Monitoring Stations 4
Table 2. Average Coordinates of Vertical Profiles during the January 2006 Survey..... 7
Table 3. Instrumental Specifications for CTD Profiler..... 11
Table 4. Discharge-Related Water-Property Anomalies 16

INTRODUCTION

The City of Morro Bay and the Cayucos Sanitary District (MBCSD) jointly own the wastewater treatment plant operated by the City of Morro Bay. A National Pollutant Discharge Elimination System (NPDES) permit, modifying secondary treatment requirements, was issued to the City of Morro Bay and the Cayucos Sanitary District in December 1998 (Permit No. CA0047881). The permit was issued by Region 9 of the Environmental Protection Agency (EPA) and the Central Coast California Regional Water Quality Control Board (RWQCB-EPA 1998a). The previous permit expired in early 1998. An administrative extension was granted through 11 December 1998 to allow time for review and issuance of a new discharge permit (RWQCB 1998).

As part of the new permit provisions, the previous monitoring program was modified to better evaluate short- and long-term effects of the discharge on receiving waters, benthic sediments, and infaunal communities (RWQCB-EPA 1998b). The program continued to include a requirement for receiving-water-quality monitoring performed on a seasonal basis. Four quarterly surveys were intended to record ambient water properties that approximate winter, spring, summer, and fall conditions. In keeping with seasonal synopses, this quarterly report summarizes the results of water-quality sampling conducted on 17 January 2006. Specifically, this first-quarter survey was conducted in January to capture ambient oceanographic conditions along the central California coast during the winter season.

The water-quality surveys also provide timely assessments of the performance of the diffuser structure in dispersing wastewater within highly stratified receiving waters. Any significant, recent damage to the diffuser structure would be revealed by a decline in the level of wastewater dispersion measured in this survey compared to that of prior surveys, and compared to design specifications. As described in this report, no such decline was observed.

Both monitoring objectives were achieved through an evaluation of the water-column profiles and vertical sections of water-property distributions that are presented in Appendix A. Appendix B tabulates instrumental measurements and standard field observations. These data were used to assess compliance with the objectives of the California Ocean Plan (COP) as specified in the NPDES discharge permit.

The January 2006 field survey was the twenty-ninth receiving-water survey to be conducted under the monitoring provisions of the current permit. Compared to the previous permit, the number of stations increased from 11 to 16, and the stations were relocated closer (≤ 100 m) to the diffuser structure. Sampling at these more closely spaced stations could only be achieved because of the availability of increased navigational accuracy that resulted from implementation of the differential global positioning satellite (DGPS) system. This system was commissioned during the March 1998 survey (MRS 1998a) and was subsequently employed in the precise determination of the open section of the diffuser structure during a diver survey on 29 September 1998 (MRS 1998bc).

The current sampling design also allowed surveying to be conducted more rapidly than previous surveys by eliminating the requirement for the time-consuming collection of discrete water samples using Niskin bottles. Continuous deployment of the CTD¹ instrument package between stations now provides a more synoptic snapshot of the water properties immediately surrounding the diffuser structure. Consequently,

¹ Conductivity, Temperature, and Depth (CTD) were the original measurements recorded by this standard oceanographic instrument package, but the moniker now connotes an electronic instrument package with a broader suite of probes and sensors capable of *in situ* measurement of dissolved oxygen, transmissivity, and pH.

the extent of the effluent plume and the amplitude of its associated water-property anomalies can be more precisely determined. The highly sensitive sensors in the CTD instrument package are capable of detecting minute changes in water properties. These sensors are described in the Methods section below.

Surveys conducted prior to 1999 rarely detected the effluent plume because sampling stations were too widely separated to resolve the dilute wastewater signature that is highly localized around the outfall diffuser. With the implementation of the current sampling design in 1999, the presence of well-mixed effluent near the diffuser structure was found in all 29 of the subsequent water-quality surveys (MRS 2000, 2001, 2002, 2003, 2004, 2005, 2006), including the one described in this report. Moreover, improved navigation in concert with the denser sampling pattern more precisely delineated the location of the discharge-related perturbations in seawater properties.

Precision navigation is important for assessing compliance because most receiving-water limitations apply only beyond the narrow zone of initial dilution that surrounds the outfall. Additionally, the amplitudes of the effluent-related perturbations can be better determined by the denser sampling pattern. The amplitudes of discharge-related salinity anomalies reveal the details of dilution as the effluent plume disperses within receiving waters. Measured dilution factors lend insight into the current operational performance of the outfall and diffuser structure. As described in this report, the presence of dilute effluent undergoing turbulent mixing close to the diffuser structure was clearly delineated by the data collected during the January 2006 survey.

STATION LOCATIONS

The water-sampling stations surround the area where effluent is discharged within Estero Bay (Figure 1). The 1,450 m long outfall pipe, which carries the effluent from the onshore treatment plant, terminates at the diffuser structure, which lies on the seafloor approximately 827 m from the shoreline². The diffuser structure itself extends an additional 52 m toward the northwest from the outfall terminus.

Twenty-eight of the 34 available ports discharge effluent along a 42 m section of the diffuser structure. The remaining six diffuser ports remain closed to improve dispersion by increasing the ejection velocity from the remaining ports. For a given flow rate, the diffuser ports were hydraulically designed to create an ejection jet, which serves to rapidly mix effluent with receiving seawater immediately upon discharge. Additional turbulent mixing occurs as the buoyant plume of dilute effluent rises through the water column. Most of this buoyancy-induced mixing occurs within a zone of initial dilution (ZID), whose lateral extent is somewhat arbitrarily defined to be approximately 15 m from the centerline of the diffuser structure.

² This distance was determined from a navigational survey conducted on 6 July 2005 to benchmark the locations of the current surfzone sampling stations along the shoreline adjacent to the diffuser structure. The beginning of the section of the diffuser structure containing open diffuser ports lies directly offshore surfzone Station C (Figure 1). This closest-approach shoreline position was determined at the water's edge when the tidal level was +2.7 ft, referenced to mean lower low water (MLLW).



Figure 1. Regional Setting of Receiving-Water Sampling Stations within Estero Bay

Beyond the ZID, the energetic waves, tides, and coastal currents within Estero Bay further disperse the discharge plume within the open-ocean receiving waters. Areas of special concern, such as sanctuaries and estuaries, are too distant to be affected by the effluent discharge. For example, the southern boundary of the Monterey Bay National Marine Sanctuary is located 38 km to the north, near Cambria Rock. Similarly, although the entrance to the Morro Bay National Estuary lies only 2.8 km to the south of the discharge, direct seawater exchange between the discharge point and the Bay is restricted by the southerly orientation of the mouth of the Bay, and by the presence of Morro Rock. Morro Rock is the largest physiographic feature of the adjacent coastline and extends into Estero Bay approximately 2 km south of the point of discharge (Figure 1). Its presence blocks the direct incursion of unmixed wastewater into the Bay.

Near the diffuser, prevailing currents generally follow bathymetric contours, which parallel the north-south trend of the adjacent coastline. Because of rapid initial mixing achieved within 15 m of the diffuser structure, impingement of unmixed effluent onto the adjacent coastline 827 m away is highly unlikely.

Nevertheless, water samples are regularly collected along the shoreline at the surfzone sampling stations shown in Figure 1. These surfzone samples are analyzed for total and fecal coliform levels. Results of these analyses are reported in monthly operational summaries and in annual reports. The occasional instances of elevated beach coliform levels result from onshore non-point sources rather than the discharge of disinfected wastewater from the MBCSD outfall (MRS 2000, 2001, 2002, 2003, 2004, 2005, 2006).

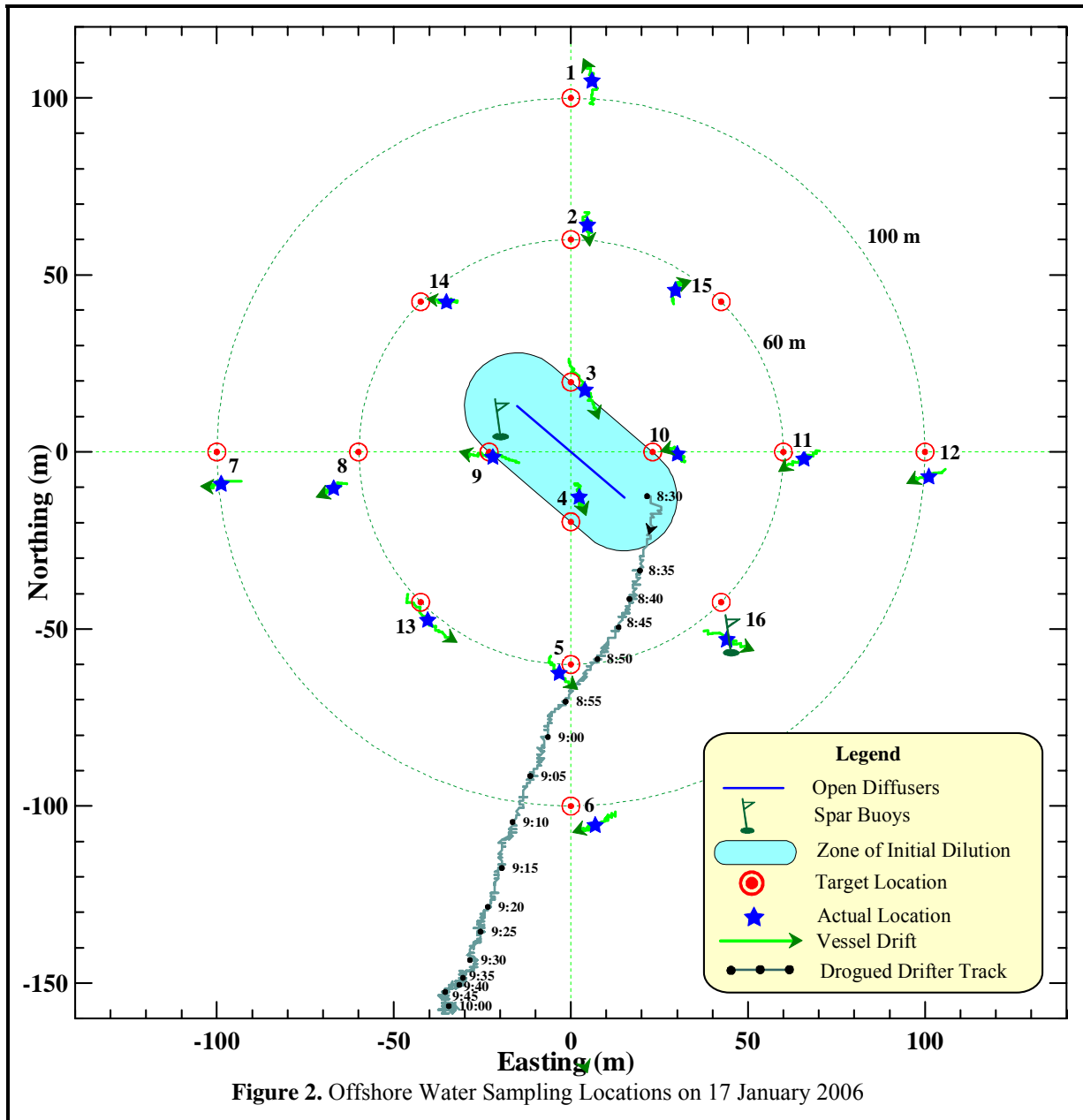
As shown in Figure 2, the water-sampling design consists of 16 fixed offshore stations located within 100 m of the outfall diffuser structure. The target locations of the 16 offshore sampling stations are indicated by the red ⊙ symbols in the Figure. Stations are situated at three distances relative to the center of the diffuser structure to capture any discharge-related trends in water properties. Six of the stations lie along a north-south axis at the same water depth (15.2 m) as the diffuser centroid. Stations 3 and 4 are positioned at the upcoast and downcoast boundaries of the ZID, at a distance of 15 m from the closest diffuser ports (Table 1). Stations 2 and 5 are located at nearfield distances (60 m) from the diffuser centroid. Stations 1 and 6 represent reference stations and are situated 100 m upcoast and downcoast of the centroid. Depending on the direction of the local oceanic currents at the time of sampling, one or more of these near and midfield stations could conceivably be influenced by the discharge. Under those circumstances, the midfield station on the opposite side of the diffuser can act as a reference station.

Table 1. Description of Receiving-Water Monitoring Stations

Station	Description	Latitude	Longitude	Closest Approach Distance ¹ (m)	Center Distance ² (m)
1	Upcoast Midfield	35° 23.253' N	120° 52.504' W	88.4	100
2	Upcoast Nearfield	35° 23.231' N	120° 52.504' W	49.4	60
3	Upcoast ZID	35° 23.210' N	120° 52.504' W	15.0	20
4	Downcoast ZID	35° 23.188' N	120° 52.504' W	15.0	20
5	Downcoast Nearfield	35° 23.167' N	120° 52.504' W	49.4	60
6	Downcoast Midfield	35° 23.145' N	120° 52.504' W	88.4	100
7	Offshore Midfield	35° 23.199' N	120° 52.570' W	85.8	100
8	Offshore Nearfield	35° 23.199' N	120° 52.544' W	46.7	60
9	Offshore ZID	35° 23.199' N	120° 52.519' W	15.0	23
10	Shoreward ZID	35° 23.199' N	120° 52.489' W	15.0	23
11	Shoreward Nearfield	35° 23.199' N	120° 52.464' W	46.7	60
12	Shoreward Midfield	35° 23.199' N	120° 52.438' W	85.8	100
13	Southwest Nearfield	35° 23.176' N	120° 52.532' W	59.8	60
14	Northwest Nearfield	35° 23.222' N	120° 52.532' W	40.2	60
15	Northeast Nearfield	35° 23.222' N	120° 52.476' W	59.8	60
16	Southeast Nearfield	35° 23.176' N	120° 52.476' W	40.2	60

¹Distance to the closest open diffuser port.

²Distance to the center of open diffuser section.



Comparisons of water properties at these antipodal stations quantify departures from ambient seawater properties so that compliance with the NPDES discharge permit can be evaluated.

Six other stations (7 through 12) were aligned along a cross-shore transect in a pattern matching that of the along-shore transect. The four additional nearfield stations (13 through 16) measure the nearfield influence of effluent transported by ocean currents flowing at oblique angles to the bathymetry.

Although the discharge is considered a ‘point source,’ it does not occur at a point of infinitesimal size. Instead, the discharge is distributed along a 42 m section of the seafloor. This finite size is an important consideration when assessing wastewater dispersion close to the discharge. Because of the finite length of

the discharge, the amount of wastewater dispersion at a given point in the water column is dictated by its distance to the closest diffuser port, rather than its distance to the center of the diffuser structure. Because of the finite size of the source, this ‘*closest approach*’ distance is considerably less than the centerline distance normally cited in modeling studies (Table 1).

Station positioning within the compact sampling pattern specified in the current permit became feasible only after the advent of DGPS. The accuracy of traditional navigation systems such as LORAN or standard GPS is typically ± 15 m, a span equal to half the total width of the ZID itself. Prior to 2 May 2000, standard commercial GPS receivers were not allowed to be perfectly accurate by law; and a built-in error system called Selective Availability (SA) was encoded into GPS transmissions. SA could introduce a misreading of up to 100 m, although it altered most measurements by less than 30 m. After May 2000, SA was turned off and the accuracy of standard GPS receivers improved substantially, with horizontal position errors of typically less than 10 m.

Nevertheless, extreme atmospheric conditions and physiographic obstructions cause signals to bounce around, leading to errors in position beyond those that were previously introduced by SA. These other errors are greatly reduced with the Differential GPS (DGPS) system that was first implemented by the U.S. Coast Guard. DGPS incorporates a second signal from a nearby land-based beacon. Because the beacon is fixed at a known location, the position error in the reading from the GPS satellites can be precisely calculated at any given time. This correction is continuously transmitted to the DGPS receiver onboard the survey vessel and results in extremely stable and accurate offshore navigation, typically with position errors of less than 2 m.

At the beginning of 1998, the survey vessel F/V *Bonnie Marietta* was fitted with a Furuno™ GPS 30 and FBX2 differential beacon receiver. This navigational system was used on 29 July 1998 to precisely locate the position of the open section of the diffuser structure (MRS 1998b) and establish the new target locations for the receiving-water monitoring stations shown in Figure 2 and listed in Table 1.

DGPS allows precise determination of sampling locations during individual water-quality surveys. Knowledge of the precise location of the actual sampling sites relative to the diffuser position is crucial for accurate interpretation of the water-property fields. During any given survey, the actual sampling locations do not coincide with the exact target coordinates listed in Table 1. Winds, waves, and currents induce offsets during sampling. Using DGPS, these offsets can be resolved and the vessel location can be precisely tracked during sampling at each station. This is an important consideration because vertical profiling conducted at an individual station can cover a large horizontal distance relative to the ZID. The magnitude of this horizontal drift is apparent in Figure 2 from the length of the green tracklines. These tracklines trace the horizontal location of the CTD instrument package as it was lowered to the seafloor at each station.

The CTD tracklines shown in Figure 2 reveal that a moderate amount of lateral drift occurred during the vertical casts at most stations. During the time it took the CTD to traverse the water column to the seafloor, which averaged 1m 12s, the instrument package moved an average of 10.0 m laterally. At stations close to the diffuser structure, this horizontal drift in the position of the CTD complicates the assessment of compliance with discharge limitations. Receiving-water limitations specified in the COP only apply to measurements recorded beyond the ZID boundary. Within the ZID, rapid turbulent mixing associated with the momentum of the effluent jet and the rise of the buoyant plume is expected, and the limitations apply to conditions after this initial mixing has occurred. The vertical casts at Stations 3 and 9 traversed the boundary of the ZID. Strictly speaking, only a portion of the data recorded during those casts is subject to the receiving-water limitations specified in the NPDES discharge permit. Additionally,

none of the measurements recorded at Station 4 are subject to the limitations because the CTD was well within the ZID boundary throughout the entire vertical cast at that station.

Compliance assessments notwithstanding, measurements recorded close to the diffuser structure within the ZID lend valuable insight into the outfall's effectiveness at dispersing wastewater during this particular survey. Damaged or broken diffuser ports would be reflected by low dilution rates and measurements of concentrated effluent throughout ZID. Without measurements recorded within the ZID, the discharge plume would probably go undetected. This was the case in nearly every water-quality survey conducted prior to 1999, before the denser sampling pattern now in use was instituted.

Surveys prior to 1999 also predated the advent of DGPS. Consequently, the 10 m average drift experienced during sampling at individual stations would not have been fully resolved with the navigation available at the time. In fact, before 1999 sampling was presumed to occur at a single, imprecisely determined, horizontal location near each station. For consistency with past surveys, a single reportable sampling location was also determined for each station during the January 2006 survey. These were based on the average location as shown by the blue stars in Figure 2. Average positions are also listed in Table 2, along with their distance from the diffuser structure. However, based on the foregoing discussion, the distance between the average station position and the ZID does not determine whether all the measurements at that station are subject to the receiving-water objectives in the discharge permit. For example, the 16 m closest-approach distance specified for Station 3 would suggest that all of the data at that station was collected outside of the ZID. In reality, as shown by the green trackline in Figure 2, the deeper measurements at Station 3 were recorded within the ZID, where water-quality limitations do not apply.

Table 2. Average Coordinates of Vertical Profiles during the January 2006 Survey

Station	Time (PST)		Latitude	Longitude	Closest Approach	
	Downcast	Upcast			Range ¹ (m)	Bearing ² (°T)
1	9:44:41	9:46:03	35° 23.256' N	120° 52.500' W	94.4	13
2	9:48:26	9:49:31	35° 23.234' N	120° 52.501' W	55.0	21
3	9:51:25	9:52:33	35° 23.209' N	120° 52.501' W	16.0 ³	41
4	9:54:06	9:55:21	35° 23.192' N	120° 52.502' W	8.0 ⁴	221
5	9:57:39	9:58:41	35° 23.165' N	120° 52.506' W	52.7	200
6	10:01:00	10:02:23	35° 23.142' N	120° 52.499' W	92.6	185
7	9:08:16	9:09:36	35° 23.194' N	120° 52.569' W	86.4	255
8	9:03:21	9:04:50	35° 23.194' N	120° 52.548' W	56.7	246
9	9:00:13	9:01:30	35° 23.198' N	120° 52.519' W	15.3 ³	221
10	8:56:38	8:57:50	35° 23.199' N	120° 52.484' W	19.5	50
11	8:53:31	8:54:39	35° 23.198' N	120° 52.461' W	51.9	78
12	8:51:01	8:51:49	35° 23.195' N	120° 52.437' W	86.2	86
13	9:13:18	9:14:37	35° 23.173' N	120° 52.531' W	62.2	221
14	9:28:09	9:29:16	35° 23.222' N	120° 52.527' W	35.7	326
15	9:23:12	9:24:22	35° 23.224' N	120° 52.484' W	54.1	41
16	9:16:45	9:17:58	35° 23.170' N	120° 52.475' W	49.2	144

¹ Distance from the closest open diffuser port. Observations collected within the ZID shown in bold

² Direction measured clockwise in degrees from true north from the closest diffuser port to the actual sampling location.

³ Portions of the CTD (Conductivity-Temperature-Depth) cast were within the ZID boundary.

⁴ All of the CTD cast was within the ZID boundary.

The vessel drift indicated by the green tracklines in Figure 2 was dictated by the complex interaction between surface currents, wind forces, and residual vessel momentum remaining after station approach. As summarized in Table B-8, winds were light and variable, but were generally offshore throughout the survey. These winds, combined with oceanic currents directed toward the south, resulted in a southwestward drift at many of the stations during the January 2006 survey.

The moderate southward current flow that prevailed during the January 2006 survey was documented by the satellite-tracked drifter, whose path is shown by the grey line with black dots in Figure 3. The drifter is designed to track the subsurface current, with little influence from the wind. Each dot along the drifter trackline represents a time span of five minutes. The drogued drifter was deployed just east of the diffuser structure at 08:30. The drifter was recovered an hour and a half later, at 10:00 PST. It had traveled 154 m toward the southwest (200° T) at an average speed of 2.8 cm/s or 0.05 knots. However, changes in the spacing of the time stamps on the trackline in Figure 2 show that the drifter slowed considerably toward the end of the survey. In the first hour, between 08:30 and 09:30, the drifter traveled at a speed of 4.0 cm/s and covered about 140 m of the trackline. In the last half hour, the drifter only moved 14 m at a speed of 0.7 cm/s.

The moderate southward flow that was measured by the drogued drifter was inconsistent with the

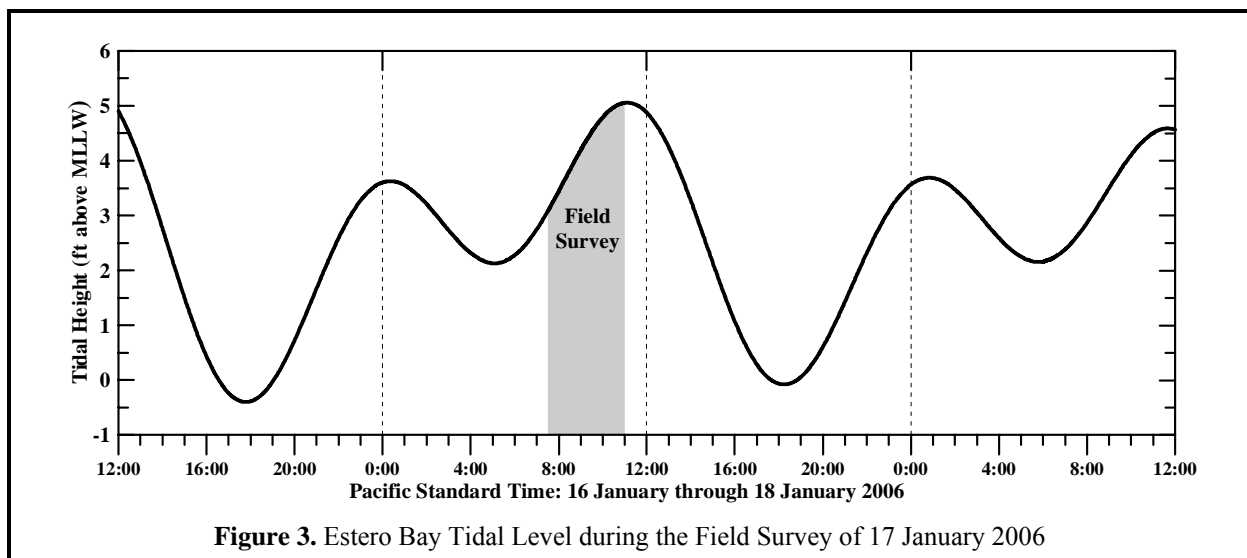


Figure 3. Estero Bay Tidal Level during the Field Survey of 17 January 2006

incoming (flood) tide that prevailed during the survey (Figure 3). In the absence of external influences, a flood tide normally induces a weak northeastward flow in the survey region. However, the flow is often also influenced by external processes, such as wind-generated upwelling. Moderate upwelling conditions prevailed throughout January, and were present around the time of the survey as seen in the satellite image on the cover of this report. The image was recorded three days after the survey when skies were clear enough for sea-surface temperatures to be measured by infrared sensors on one of NOAA's polar orbiting satellites.

The moderate upwelling that occurred around the time of the survey was largely responsible for the water-column stratification that is evident in most of the vertical profiles recorded with the CTD (Figures A-1 through A-3 in Appendix A). Upwelling season normally begins sometime during late March and or

early April when there is a “spring transition” to more persistent southward-directed winds along the central California coast. However, these southward-directed winds were also prevalent during January 2006. The spring transition is marked by the stabilization of a high atmospheric pressure field over the northeastern Pacific Ocean. Clockwise winds around this pressure field drive the prevailing northwesterly winds along the central coast. The prevailing winds move surface waters southward and offshore. To replace these coastal surface waters, deep, cool, nutrient-rich waters upwell near the coast. The cool upwelled water is delineated in the cover image with blue (12.5°C) and purple (11.5°C) water along the shoreline. At major promontories, this upwelled water extends well offshore of the coast. The satellite image shows that because of coastal upwelling, sea-surface temperatures were near or below 12°C within Estero Bay. This is consistent with the near-surface temperatures measured by the CTD during the survey, which were around 12.2°C as shown in Table B-1 in Appendix B.

The nutrient-rich seawater that is brought to the sea surface by upwelling enables phytoplanktonic blooms that are the foundation of the productive marine fishery found along the central California coast. The cross-shore flow associated with persistent upwelling conditions also leads to vertical stratification of the water column. The resulting deep (>10 m) thermocline is commonly maintained throughout the summer and into the fall. In contrast, winter oceanographic conditions are generally characterized by a vertically uniform water column that has been well mixed by intense winds generated by passing local storm fronts and large waves produced in distant Pacific storms. This was not the case during the January 2006 survey when, instead, upwelling winds prevailed along the central coast.

METHODS

The 38 ft F/V *Bonnie Marietta*, owned and operated by Captain Mark Tognazzini of Morro Bay, served as the survey vessel on 17 January 2006. Dr. Douglas Coats and Ms. Bonnie Luke of Marine Research Specialists (MRS) provided scientific support. Captain Mark Tognazzini supervised vessel operations, while Mr. Marc Tognazzini acted as marine technician. Secchi depth measurements and standard observations for weather, seas, water clarity/coloration, and the presence of any odors, floating debris, and oil and grease were recorded during the survey. Wind speeds and air temperatures were measured with a Kestrel[®] 2000 Thermo-Anemometer. These ancillary observations were collected during the rapid water-column profiling that was conducted at each station using a CTD instrument package.

Ancillary Measurements

At all stations, a Secchi disk was lowered through the water column to determine its depth of disappearance (Table B-8). Secchi depths provide a visual measure of near-surface turbidity or water clarity. The depth of disappearance is inversely proportional to the average amount of organic and inorganic suspended material along a line of sight in the upper water column. As such, the Secchi depth measures natural light penetration, which can be limited by increased suspended particulate loads from plankton blooms, onshore runoff, seafloor resuspension, and wastewater discharge. It is also of biological significance because the depth of the euphotic zone, where most oceanic photosynthesis occurs, extends to approximately twice the Secchi depth. Secchi depths of between 3 m and 4 m that were observed during the January 2006 survey are typical of upwelling conditions when increased primary productivity normally results in decreased light transmissivity in the upper water column.

Secchi depths are less precise than measurements recorded by the transmissometer mounted on the CTD instrument package. For example, the visibility of the disk, and hence its depth of disappearance, depends on the amount of natural light available at the time of the measurement. Thus, the Secchi depth reading

can artificially change by as much as 0.5 m depending on whether the sample is taken on the sunny or shady side of the boat. Moreover, a temporal drift in the measurements can be introduced as the sun rises in the sky while the survey progresses. Nevertheless, Secchi depth measurements reflect general turbidity levels within the upper portion of the water column, including waters within a meter of the sea surface where, because of the physical size of the CTD package, the transmissometer cannot record turbidity.

During the January 2006 survey, a satellite-tracked drifter was deployed near the open section of the diffuser structure. The drifter was drogued at mid-depth (7 m) using the curtain-shade design of Davis et al (1982). In this configuration, the drifter's trajectory was largely dictated by the oceanic flow field rather than by surface winds. The time and precise position of the drifter deployment and recovery were recorded. The January 2006 survey was the fifth MBCSD survey to continuously record the drifter position throughout its deployment. In the past, the average ambient flow velocity during each survey was estimated solely from the deployment and recovery positions. However, during the January 2006 survey, the added satellite-tracking capability of the drifter revealed some curvature in the path of the drifter and changes in its speed as shown in Figure 2. Drifter data collected in most prior surveys lacked information on this and other short-term flow fluctuations that can occur within the duration of a survey.

Instrumental Measurements

Vertical water-column profiling was conducted using an electronic instrument package equipped with a number of probes and sensors. A Sea Bird Electronics SBE-19 Seacat CTD package was used to collect profiles of conductivity, salinity, temperature, light transmittance, dissolved oxygen (DO), pH, density, and pressure at each station. A submersible pump on the CTD continuously flushed water through the conductivity cell and oxygen plenum at a constant rate, independent of the CTD's motion through the water column. After the October 2001 survey, the CTD was returned to the factory for full testing, repair, and calibration. Temporal drifts in the oxygen and alkalinity readings during the October 2001 survey indicated that the sensitivity of these probes had degraded because of an accumulation of marine growth. During the factory repair, the pH probe was replaced and the electrolyte in the oxygen sensor was refurbished. The entire CTD system was then recalibrated at the factory. Upon return of the instrument, the transmissivity, dissolved oxygen, and pH sensors were recalibrated at the MRS laboratory. Calibration coefficients determined at the factory and by MRS were nearly identical, and confirmed the accuracy and stability of the refurbished sensors.

The DO and pH sensors were again returned to the factory in May 2003 for testing and recalibration. Because of increasing temporal drift associated with the aging DO probe, it was replaced with a new DO probe. As is the case before all surveys, the CTD system was recalibrated at the MRS laboratory prior to the January 2006 survey. Calibration at upper-bound DO concentrations was established by immersing the CTD in an aerated, temperature-controlled calibration tank. In addition to oxygen readings at full saturation, a zero-oxygen calibration point was determined by filling the oxygen-sensor plenum with an 8% solution of sodium sulfite (Na_2SO_3). Oxygen calibration coefficients were determined by regression analysis of sensor-membrane current and temperature, as recommended by the manufacturer (SBE 1993). As with prior factory calibrations, pre-cruise calibration coefficients determined by MRS closely corresponded to those determined by the factory.

Prolonged equilibration times of the pH sensor has been an ongoing challenge that has required removal of temporal trends in the pH data collected in most surveys, even those following the pH-sensor replacement. Laboratory tests conducted in conjunction with pre-cruise calibrations have demonstrated that the equilibration time is reduced if the sensor is immersed in water prior to deployment. This was accomplished during the January 2006 survey by attaching a water-filled hose to the sensor during transit

to the survey area. Immediately prior to deployment, the hose was removed. Although this procedure did not entirely eliminate the temporal offsets, it markedly reduced their amplitude. The required pH adjustments were small, and did not exceed 0.027 pH units.

During the pre-cruise calibration, coefficients for the pH (alkalinity) sensor were determined from a linear regression of output voltage after immersion in three separate buffered solutions of known pH. Buffering solutions with a pH of 4 ± 0.01 , 7 ± 0.01 , 8 ± 0.01 and 10 ± 0.02 were used to bracket the range of in situ measurements. The SeaTech transmissometer was air calibrated by fitting the voltages recorded with and without blocking of the light transmission path in air, as recommended by the manufacturer (SBE 1989). Revised calibration coefficients determined prior to the survey were used in the algorithms that convert sensor voltage to engineering units when the field data were processed. Comparison with the factory calibration of the entire CTD package that was conducted in December 2001 confirmed the continued accuracy and stability of the temperature, pressure, and conductivity sensors, as well as the operational integrity of the oxygen and pH probes.

Six seawater properties were used to assess receiving-water quality in this report. They were derived from the continuously recorded output from the probes and sensors on the CTD. Depth limitations on the combination oxygen/pH sensor confine the CTD to depths less than 200 m (Table 3), which is well beyond the maximum depth of the deepest station in the outfall survey. The precision and accuracy of the various probes, as reported in manufacturer's specifications, are also listed in the Table. Salinity (‰) was calculated from conductivity (Siemens/m) measurements. Density was derived from contemporaneous temperature (°C) and salinity data. It was expressed as 1000 times the specific gravity minus one, which is a unit of sigma-T (σ_t).

All three of these physical parameters (salinity, temperature, and density) were used to determine the lateral extent of the effluent plume. Additionally, they define the layering (vertical stratification) of the receiving waters, which determines the behavior and dynamics of the wastewater as it mixes with seawater within the ZID. Data on three remaining seawater properties, consisting of light transmittance (water clarity), hydrogen-ion concentration (acidity/alkalinity – pH), and dissolved oxygen (DO), further characterize receiving waters, and were used to assess compliance with water-quality criteria. Light transmittance was measured as a percentage of the transmitted beam of light detected at the opposite end of a 0.25 m path. Increased transmittance indicates increased water clarity and decreased turbidity.

Table 3. Instrumental Specifications for CTD Profiler

Component	Depth¹	Units	Range	Accuracy	Resolution
Housing	600	—	—	—	—
Pump	3400	—	—	—	—
Pressure	680	Psia	0 to 1000	± 5.0	± 0.5
Depth	—	Meters	0 to 690	± 3.0	± 0.3
Conductivity	600	Siemens/m	0 to 6.5	± 0.001	± 0.0001
Salinity	600	‰	0 to 38	± 0.006	± 0.0006
Temperature	600	°C	-5 to 35	± 0.01	± 0.001
Transmissivity	2000	%	0 to 100	± 0.1	± 0.025
Dissolved Oxygen	200	mg/L	0 to 21.5	± 0.14	± 0.014
Acidity/Alkalinity	200	pH	0 to 14	± 0.1	± 0.006

¹Maximum depth limit in meters

Before deployment at the initial station, the CTD was held below the sea surface for an eight-minute equilibration period. Subsequently, the CTD was raised to within 1.0 m of the sea surface and profiling commenced. The CTD was lowered at a continuous rate of speed to the seafloor. Measurements at multiple stations were collected during each deployment by towing the CTD package below the water surface while transiting between adjacent stations. Upon retrieval of the CTD, the profile data were downloaded to a portable computer.

Temporal Trends in the pH Sensor

The pH sensor exhibited a slight temporal drift during the January 2006 survey. Perceptible drift in pH measurements has been consistently observed in prior water-quality surveys as the result of ongoing sensor equilibration during profiling. Prolonged exposure to the atmosphere between surveys results in the largest offsets and can also affect the dynamic range of the measurements. Smaller equilibration offsets have been observed when the CTD is redeployed after being brought onboard to download data during the middle of the survey. Previous attempts to mitigate sensor drift have included prolonging the soak time of the CTD after deployment below the sea surface prior to profiling. Soak times in excess of six minutes at the beginning of a survey were found to reduce but not entirely eliminate sensor drift. During the January 2006 survey, a tube filled with seawater was placed around the pH sensor to limit atmospheric exposure before the CTD was first deployed. This technique was successful at further ameliorating sensor drift.

Temporal drift in the pH sensor was responsible for slight, but perceptibly lower pH measurements at those stations occupied during the beginning of the CTD deployment. The pH measurements at the first station (12) averaged 0.027 pH units lower than the measurements recorded later in the deployments. Comparison with Table 3 shows that this artificial reduction in measured pH is smaller than the instrumental accuracy (± 0.1 pH). However, it is larger than the instrumental resolution (± 0.006 pH). As a result, slight artificial differences are embedded in the measurements reported at Stations 11 and 12 in Table B-7. Stations 11 and 12 were the first stations occupied during the survey and required the largest adjustment for sensor drift. Temporal detrending at these and other stations removed these instrumental anomalies, and the results are tabulated in Table B-6.

RESULTS

The water-quality survey for the first quarter of 2006 began on Wednesday, 17 January 2006, at 08:30 PST with the deployment of the drogued drifter. Subsequently, all water-column measurements were collected as required by the NPDES monitoring program (Table 2 and B-8). Sunrise was at 07:11 PST and skies were hazy throughout the survey, which ended at 10:40 PST when the vessel arrived back at port. Average wind speeds, calculated over one-minute intervals, were light and variable throughout the survey and ranged from approximately 0.3 kt to 3.3 kt, with peak speeds ranging from 0.8 kt to 4.0 kt. A 1 ft swell moved through the survey area from the west. Atmospheric visibility was greater than 2 nM along the ocean surface owing to the absence of low-lying fog. Morro Rock and the shoreline remained visible throughout the survey. Air temperature increased from 14°C to 18°C during the course of the survey. The surface seawater temperature (12.2°C) in the survey area was notably cooler than the average air temperature, and was consistent with coastal sea-surface temperatures within Estero Bay recorded by the satellite image shown on the cover of this report.

The discharge plume was not readily visible near the sea surface during the survey. However, at times, slightly different shading near Stations 4 and 5 may have reflected the surfacing plume. This location is

consistent with the southward flow at the time of the survey. A surfacing plume at those stations is also consistent with instrumental observations and the plume's near-surface presence at Station 4 may account for the slightly shallower Secchi depth (3 m) measured there, as compared with the 4 m depths recorded at other stations (Table B-8). Throughout the survey, there was no visual evidence of floating particulates, oil and grease, or seawater discoloration associated with the discharge.

Beneficial Use

During the January 2006 survey, observations of beneficial use demonstrated that the coastal waters in the outfall vicinity continued to be utilized by wildlife and for recreation. A whale spout, possibly from a blue whale (*Balaenoptera musculus*), was observed well offshore of the survey area during transit from the Morro Bay harbor to the monitoring area. Surf scoters (*Melanitta perspicillata*), and western gulls (*Larus occidentalis*) were observed transiting through and resting near the survey area. Surf scoters are common along the Pacific coast in late winter and usually stay some distance from shore, feeding on shellfish. The males are distinguished by a bright red-orange pattern on their bill. Additionally, pedestrians were observed throughout the survey walking and jogging along Morro Strand State Beach, and a surfer was observed at the break north of Morro Rock. No other evidence of beneficial use of receiving waters was noted during the survey.

Ambient Seawater Properties

Data collected during the January 2006 survey reflect the classical, stratified conditions that are indicative of upwelling. Upwelling results in an influx of dense, cold, saline water at depth and often leads to a sharp thermocline, halocline, and pycnocline where temperature, salinity, and density change rapidly over short vertical distances. Under stratified conditions, isotherms crowd together to form a thermocline that restricts the vertical transport of the effluent plume and reduces its dispersion.

Moderate upwelling-induced vertical gradients are marginally apparent throughout the water column in most of the vertical profiles shown in Figures A-1 through A-3. A thermocline, where temperature steadily decreases with increasing depth, is evident in nearly all of the vertical profiles shown in Figures A-1 through A-3 (red lines). As described in the following sections, a sharper shallow thermocline was apparent at Stations 4, 5, and possibly 6 because the effluent discharge altered the vertical structure of the water column. However, at the other stations some ambient seawater properties exhibited vertical stratification nearly identical to that of the thermal structure. For example, the shape of the temperature profile at any given station is closely reflected in the pH profiles (olive lines). Similarly, the steady decrease in temperature pH with depth are mirrored by a pycnocline, where density (black lines) increases steadily with depth, and a halocline, where salinity (bright green lines) also increases with depth.

The ambient vertical structure of the two remaining seawater properties, dissolved oxygen (DO-dark blue lines) and transmissivity (light-blue lines), departed from the steady increase or decrease seen in the other properties. In particular, DO concentrations were relatively uniform at 7.5 mg/L down to a depth of approximately 9 m at most stations. Below that depth DO exhibited a sharp decrease down to approximately 6 mg/L within a 3-m depth span. This sharp oxygen gradient coincided with a sharp increase in transmissivity suggesting that there was a distinctly different water mass present in the lower half of the water column. This low-oxygen, low-turbidity water mass was characterized by comparatively high salinities and originated from deep offshore areas. It moved shoreward to replace near-surface seawater that was transported offshore by upwelling.

Large-scale features of the upwelling process within Estero Bay were previously described by MRS (2005) and Morro Group, Inc. (2000). Near the seafloor, upwelling transports cold, dense seawater shoreward to replace nearshore surface waters that are driven offshore by prevailing winds. The low DO found at depth is a clear indicator of its deep offshore origin. Deep offshore waters are undersaturated in oxygen because they have not had direct contact with the atmosphere for long periods of time, and biotic respiration and decomposition have slowly depleted the dissolved-oxygen levels. Similarly, slightly elevated salinity is often indicative of waters that originate in the Southern California Bight and are carried northward by the Davidson undercurrent. These waters differ from the relatively fresh surface water associated with the southward-flowing California Current.

Vertical profiles of transmissivity (light-blue lines) exhibit a much more complex “S” shape that markedly departs from the steadily increasing or decreasing trends seen in other seawater properties. A variety of processes are involved in the vertical distribution of seawater turbidity. For example, during the January 2006 survey, low turbidity (high transmissivity) very close to the sea surface and at depth, sandwiched a very distinct layer of high-turbidity seawater between 5 m and 10 m. The ambient seawater properties in this layer probably reflect the increased primary productivity associated with upwelling conditions. Nutrient-rich seawater moved upward into the euphotic zone by upwelling enables phytoplanktonic blooms. Reduced water clarity (light-blue lines) above 10 m is the earmark of an increase in planktonic biomass. The enhanced primary productivity in the upper water column also produces oxygen and consumes carbon dioxide (CO₂). The removal of carbonic acid (dissolved CO₂) accounts for the higher pH found in the upper water column (olive lines). As the ratio of respiration to photosynthesis increases with depth, there is an increase in dissolved CO₂ and a concomitant decline in pH, indicating the slightly more acidic nature of the seawater. Accordingly, respiration consumes oxygen and produces acid, which accounts for the declines in DO and pH within the deeper portions of the water column as seen in Figures A-1 through A-3.

In contrast to the other water properties, transmissivity also shows a marked reduction immediately above the seafloor at many stations. The distinctive decrease in transmissivity within a thin layer immediately above the seafloor indicates the presence of a bottom nepheloid layer (BNL), which is a widespread phenomenon on continental shelves (Kuehl et al. 1996). The increased turbidity within the BNL is caused by the presence of naturally occurring particulates formed from lightweight flocs of detritus. This detritus is easily suspended by oscillatory bottom currents generated by passing surface gravity waves.

Lateral Variability

The influence of the effluent discharge can be best identified from localized anomalies in seawater properties, particularly salinity. These discharge-related anomalies are evident at Stations 4 and 5 in the along-shore vertical sections shown in Figures A-4 and A-5. In contrast to the vertical profiles, discharge-related anomalies become especially apparent in the vertical sections when seawater properties from the same depth level are compared at adjacent stations. The vertical sections also show that the shallow anomalies in temperature, transmissivity DO, and pH have the same characteristics as ambient waters at depth. They are only apparent because these deep water properties have been displaced upward into the water column where the surrounding seawater characteristics differ. Because of this, the analysis of lateral variability in seawater properties forms the basis for assessments of water-quality impacts.

In particular, the significance of each potential discharge-related anomaly is statistically evaluated by comparing its amplitude to the natural background variability. To that end, each observation at a particular station was compared with the observations from other stations at the same depth level. Measurements recorded within 10 m of the sea surface were compared with other measurements at the same depth level

below the sea surface. However, deeper measurements were compared with other measurements recorded at the same height above the sloping seafloor. This is done because deep seawater properties tend to parallel the sloping seafloor rather than the horizontal sea surface.

The statistical significance of departures from ambient seawater properties was computed from the raw CTD data listed in Tables B-1 through B-7. First, anomalies from mean conditions were computed by subtracting a particular measurement from the average of all other measurements at the same depth level, whether measured relative to the sea surface or the seafloor. Natural variability was estimated from the standard deviation of all measurements (excluding the one in question) for a given seawater parameter (e.g., salinity). Statistically significant anomalies were those that departed from mean conditions by more than the 95% confidence interval determined from the standard deviation and number of observations used to compute the average. Statistically significant departures from ambient conditions are highlighted in Tables B-1 through B-7, with bolded values enclosed in boxes.

In the January 2006 dataset, several transmissivity observations were found to be statistically significant, but were unrelated to the effluent discharge. In particular, the four deep transmissivity anomalies (Table B-5) at Stations 1, 5, 11, and 13 were artifacts of a slight variation in the thickness of the bottom nepheloid layer (BNL). Lateral variability was artificially introduced by differences in the thickness of the BNL and by proximity of the CTD samples to the seafloor; i.e., how far into the BNL the individual measurements were recorded. The 0.5-m thick BNL had slightly higher turbidity compared to waters immediately above the BNL. Consequently, the vertical sampling interval of 0.5 m spanned a significant portion of this thin layer, which lies very close to the seafloor. Also, the BNL interface is particularly sharp, so even slight variations in the thickness of the boundary layer between stations appear as “*significant*” lateral variations in transmissivity. For example, the transmissivity anomaly near the seafloor at Station 5 was a positive anomaly where transmissivity was higher than at surrounding stations because the CTD did not penetrate the turbid BNL layer at that particular station.

Even without differences in BNL measurements, the presence of statistically significant anomalies that are unrelated to the discharge is expected. From the definition of a 95% confidence level, one ‘*significant*’ departure out of every 20 measurements should occur by chance alone. With more than 500 measurements examined for each of the six parameters, it is not surprising that a few departed from the mean by an amount more than the 95% confidence interval. Moreover, when multiple hypotheses are being tested (i.e., one for each observation), the error rate for each individual test should be adjusted to achieve the overall error rate of 5% (95% confidence). By definition, this error rate is the probability that one or more of the hypothesis tests would incorrectly find a significant difference when none exists. Thus, without correcting for repeated hypothesis testing, the individual tests are conservative and “*significant*” departures will be found more often than if a single test were being performed at the 95% confidence level.

Discharge-Related Perturbations

During the January 2006 survey, three perturbations in seawater properties were unequivocally related to the discharge (Perturbations P1, P2, and P3 in Table 4). A discharge-related perturbation is a group of anomalies in one or more seawater properties that are contiguous at a particular station. The vertical distribution of seawater properties within and below the perturbations lends insight into which of two discharge processes were responsible for generating a particular anomaly. As indicated in Table 4, most of the anomalies were generated by the entrainment of naturally occurring seawater within the rising effluent plume. The connection between deep ambient seawater and the shallow anomalies is particularly apparent in the middle and bottom frames of Figure A-5.

Table 4. Discharge-Related Water-Property Anomalies^a

Perturbation ^b	Station	Depth Range	Depth of Extremum	Property	Magnitude	Process
P1 Dilution \geq 126:1	4	10.5 to 12.0 m	11.0 m	Salinity	-0.276 ‰	Effluent
		10.5 to 12.0 m	11.0 m	Density	-0.188 σ_t	Effluent
		12.0 to 15.0 m	13.5 m	Transmissivity	-11.8 ‰	Effluent/ Entrainment
P2 Dilution \geq 795:1	4	3.0 to 7.0 m	3.5 m	Salinity	-0.042 ‰	Effluent
		4.0 to 8.5 m	4.0 m	Density	+0.045 σ_t	Entrainment
		3.5 to 10.5 m	4.0 m	Temperature	-0.27 °C	Entrainment
		4.5 to 10.5 m	9.0 m	Transmissivity	+1.6 ‰	Entrainment
		3.5 to 9.5 m	5.5 m	Dissolved Oxygen	-1.3 mg/L	Entrainment
		5.5 to 10.5 m	6.5 m	pH	-0.04	Entrainment
P3 Dilution \geq 669:1	5	1.0 to 8.5 m	8.0 m	Salinity	-0.050 ‰	Effluent
		1.0 to 10.5 m	2.0 m	Density	+0.044 σ_t	Entrainment
		1.5 to 9.0 m	4.5 m	Temperature	-0.27 °C	Entrainment
		1.0 to 3.0 m	2.0 m	Transmissivity	-2.6 ‰	Entrainment
		4.5 to 11.5 m	10.0 m	Transmissivity	+16.0 ‰	Entrainment
		1.0 to 10.0 m	6.0 m	Dissolved Oxygen	-1.3 mg/L	Entrainment
		1.0 to 11.5 m	6.0 m	pH	-0.05	Entrainment

^a Anomalies shown in bold type were statistically significant

^b Perturbations consist of a group of spatially consistent anomalies in different seawater properties

In contrast, the salinity and density anomalies associated with Perturbation P1 could only have been generated by the presence of wastewater constituents. The top and bottom frames of Figure A-4 show that the portions of these anomalies near 11 m were vertically isolated. More importantly, the seawater properties within these anomalies were far different than the ambient seawater properties, even at depth. Consequently, they could not have been generated by entrainment of ambient water within the rising effluent plume. Specifically, salinities well below 33.35‰ are delineated in red in the upper frame of Figure A-4. These salinities are well below the lowest ambient salinity (33.40‰) that was measured in ambient seawater during the January 2006 survey. Ambient conditions are well-represented by the cross-shore vertical sections shown in Figures A-6 and A-7. As shown by the salinity scale in the top frame of Figure A-6, the salinity in naturally occurring seawater at depth did not drop much below 33.60‰ during the survey. Consequently, the upward movement of deep ambient seawater could not possibly account for the observed salinity anomaly associated with Perturbation P1. The same argument applies to the density anomaly observed at the same location (bottom frame of Figure A-4). These were the only significant discharge-related anomalies found during the January survey (bolded values in Table 4).

Conversely, there were many entrainment-generated anomalies found during the survey. They directly reflect ambient conditions at depth. This strongly indicates that these anomalies were produced by the upward displacement of ambient bottom water, rather than the presence of effluent constituents. Namely, these entrainment-generated anomalies were produced when ambient seawater at depth was entrained in the rising effluent plume. After being displaced upward, the differing bottom-water properties are juxtaposed with shallow-water properties, and the contrast becomes apparent as an anomaly. Figures A-6 and A-7 show that during the January 2006 survey, the presence of a deep watermass caused seawater within the deep thermocline to be naturally low in temperature, pH, and DO. The vertical sections shown in Figures A-4 and A-5 show that these low ambient seawater properties at depth are comparable to the properties observed in the anomalies within the upper water column at Stations 4 and 5.

Changes in the complex vertical structure of the transmissivity field were also diagnostic of entrainment processes. The very distinct layer of turbid seawater between 5 m and 10 m is readily apparent in the upper frame of Figure A-7. Under ambient conditions, this turbid layer was continuous and unbroken. However, less turbid seawater that was entrained within the rising effluent plume at Stations 4 and 5 created a gap in this feature as shown in the upper frame of Figure A-5. This also resulted in positive transmissivity anomalies associated with Perturbations P2 and P3 in Table 4. This means that the discharge-induced anomalies were less turbid than the surrounding seawater at depth. Clearly, this is opposite of the type of transmissivity anomaly that would be caused by the presence of heavy wastewater particulate loads. However, as the plume rose farther in the water column at Station 5, it encountered the layer of ambient water that was naturally low in turbidity. There, a second entrainment-generated transmissivity anomaly was produced; however, in this case, the anomaly was slightly negative as is listed near 2 m in Table 4. This example shows how entrainment-generated anomalies are largely controlled by the character of the ambient seawater at various depths within the water column.

Without this naturally occurring stratification, entrainment of deep ambient seawater within the rising effluent plume would not produce obvious differences between the entrained water and shallow water properties. Thus, the entrained deep seawater acts as a tracer of the effluent plume after discharge. These same entrainment-generated anomalies could just as easily have been produced by the discharge of warm seawater, containing no suspended solids or other contaminants whatsoever. Conversely, they would not be apparent in unstratified receiving waters. This indicates why many of the receiving-water limitations specified in the COP explicitly state that limitations only apply to impacts caused by the presence of wastewater constituents, and, by implication, not to changes generated by the entrainment of ambient seawater. Entrainment-generated impacts are largely dictated by existing ambient seawater stratification rather than the quality of discharged wastewater. Naturally occurring vertical differences in seawater properties are eventually mixed throughout the water column by natural nearshore processes; plume entrainment simply serves to accelerate this process within a localized area.

It is noteworthy that there were no anomalies in temperature, DO, and pH associated with the high-amplitude effluent-induced Perturbation P1. This supports the hypothesis that the properties of discharged wastewater contribute little to shallow anomalies in temperature, DO, and pH, and that they are generated instead by the upward displacement of ambient waters. There was also a moderate drop in transmissivity (-11.8%) associated with this perturbation. However, in this case, it is not clear how much of the increased turbidity was induced by the presence of wastewater particulates, and how much was generated by the entrainment of naturally turbid water within the BNL. Again this transmissivity anomaly was relatively small in amplitude, considering the close proximity of the measurement to the point of discharge. Even though it was not statistically significant, it was apparent in the upper frame of Figure A-5 only because of the consistently high ambient transmissivity (>70%) that prevailed at that depth level during the January-2006 survey.

Perturbation P1 was measured very close to the discharge and reflects effluent that was continuing to undergo rapid dilution (Station 4 in Figure 2). The large negative density anomaly associated with this perturbation (Table 4) clearly demonstrates that it was highly buoyant and would continue to rise through the water column. This is also apparent in the vertical density section shown in the bottom frame of Figure A-4. The very low-density anomaly near 11 m (delineated in red) is situated just below a water parcel of more dense seawater (shown in blue). This kind of density inversion reflects a strong buoyancy instability that is never seen under natural conditions in the ocean because they rapidly dissipate during turbulent overturn. The same process will occur with this perturbation leading to rapid additional dilution. Thus, Perturbation P1 reflects conditions within the turbulent jet shortly after discharge. It captures the early stages of the dilution process before buoyancy induced mixing has played a role in further dilution.

In contrast, the other two perturbations (P2 and P3) reflect conditions after the plume has risen through the water column and accordingly, the salinity anomalies are far smaller, and there is no evidence of a negative density anomaly. In fact, the slightly positive density anomalies associated with these perturbations are indicative of the plume reaching buoyant equilibrium.

Initial Dilution Computations

The amplitude of negative salinity anomalies at Stations 4 and 5 lends insight into effectiveness of the outfall at dispersing effluent and, ultimately, compliance with the receiving-water objectives of the COP and NPDES discharge permit. The critical initial dilution applicable to the MBCSD outfall was conservatively estimated to be 133:1 (Tetra Tech 1992). This estimate was based on worst-case modeling using highly stratified conditions where the trapping of the plume below the thermocline limited the mixing achieved during the plume's buoyant rise through the water column. That dispersion modeling determined that, after initial mixing was complete, 133 parts of ambient water would have mixed with each part of wastewater. The modeling predicted that this dilution would be achieved after the plume rose only 9 m from the seafloor, whereupon it became trapped below a thermocline and spread laterally with no further substantive dilution. A 9-m rise translates into a trapping depth 6.4 m below the sea surface.

However, as described below, computations of dilution based on the salinity anomaly within the deep perturbation at Station 4 demonstrate that the effluent plume is likely to actually achieve a far higher dilution at the predicted trapping depth. Moreover, measured dilutions exceeding 600:1 within Perturbations P2 and P4 demonstrate that the plume was not trapped at depth, and, in fact, rose to the sea surface where very high dilutions were achieved. More importantly, the deep measurements at Station 4 demonstrate that mixing within the turbulent discharge jet very close to a diffuser port achieved a dilution (126:1) comparable to the total dilution (133:1) predicted by conservative modeling. Thus, rapid mixing associated with the momentum of the discharge jet is capable of achieving the dilution levels predicted by modeling, without even considering the additional dilution that is achieved by the buoyant rise of the plume. All of this demonstrates that the diffuser structure was operating far more efficiently than predicted by the modeling.

The conservative nature of the dilution ratio determined from modeling is an important consideration because it was used to specify permit limitations on chemical concentrations in wastewater discharged from the treatment plant. These end-of-pipe effluent limitations were back-calculated from the receiving-water objectives listed in the COP (SWRCB 1997) using the 133:1 dilution ratio determined from the modeling. Use of a higher critical dilution ratio would relax the stringent end-of-pipe effluent limitations that were thought to be necessary in order to meet Ocean-Plan standards.

End-of-pipe effluent limitations are based on the definition of dilution (Fischer et al. 1979), where the concentration of a particular contaminant in effluent is given by:

$$C_e \equiv C_o + D (C_o - C_s) \quad \text{Equation 1}$$

where: C_e = the concentration of a constituent in the effluent,
 C_o = the concentration of the constituent in the ocean after dilution by D ,
 D = the dilution ratio of the volume of seawater mixed with effluent, and
 C_s = the background concentration of the constituent in ambient seawater.

The actual dilution achieved by the outfall can also be computed from Equation 1 using measured seawater anomalies. This measured dilution can then be compared with the critical dilution factor determined from modeling. Salinity is an especially useful tracer because it directly reflects the

magnitude of ongoing dilution. Specifically, the salinity concentration in effluent is negligible so C_e is eliminated in Equation 1 and the dilution ratio (D) can be computed from the salinity anomaly ($A = C_o - C_s$) as:

$$D = \frac{-C_o}{(C_o - C_s)} \equiv \frac{-C_o}{A} \quad \text{Equation 2}$$

where: D = the dilution ratio of the volume of seawater mixed with effluent,
 C_o = the salinity of the effluent-seawater mixture after dilution by D ,
 C_s = the background seawater salinity (approximately 33.6‰), and
 $A = C_o - C_s$ = the salinity anomaly.

Computed dilutions during the stratified conditions of the January 2006 survey demonstrate that the modeled dilution factors are more conservative than those actually achieved by the diffuser structure. Specifically, dilutions exceeding 669:1 were measured within the upper water column at Stations 4 and 5, across a depth range encompassing the 6.4 m trapping depth predicted by modeling. These high dilutions were determined from the largest-amplitude salinity anomalies (-0.042‰ and -0.050‰) that were observed at Stations 4 and 5 within Perturbations P2 and P3 (Table 4). Equation 2 computes a dilution ratio of 669:1 associated with the measured salinity anomaly in Perturbation P3. Smaller-amplitude salinity anomalies observed at other depth levels within Perturbations P2 and P3, which extended from 1 m to 8.5 m, yield even higher dilution ratios.

Conversely, the much larger-amplitude salinity anomalies associated with Perturbation P1 at Station 4 only extend from 10.5 m to 12.5 m. This perturbation was highly localized around the discharge point and yielded dilution ratios in excess of 126:1 (Table 4). This dilution was comparable to the final dilution (133:1) predicted by modeling after a 9 m rise of the plume through the water column, and demonstrates that the momentum of the discharge jet alone is capable of achieving dilution levels close to the permit-specified dilution ratio, without even considering the additional dilution achieved when the plume reaches equilibrium within the water column. This also explains why the discharge consistently meets receiving water limitations, and why the presence of dilute wastewater particulates is rarely detected in the upper water column, beyond the ZID.

In particular, the smallest dilution (669:1) computed from salinity data collected in the upper water column during the January 2006 survey was more than five-times higher than the 133:1 critical dilution used to establish permitted limitations on contaminant concentrations within wastewater discharged from the MBCSD treatment plant. The dilution computation demonstrates that, during the January 2006 survey, the outfall was performing better than designed, and was rapidly diluting effluent more than 660-fold. Consequently, COP receiving-water objectives were easily met by the chemical concentration limits promulgated by the NPDES discharge permit issued to the MBCSD.

DISCUSSION

Sampling during the January 2006 survey indicated that the wastewater discharge was in compliance with the receiving-water limitations specified in the NPDES permit, and with the water-quality objectives of the COP (SWRCB 1997) and the Central Coast Basin Plan (RWQCB 1994). Specifically, there were no particulates of sewage origin seen floating on the ocean surface at any of the stations sampled during the January 2006 water-quality survey and the discharge complied with all other numeric limits on seawater properties.

Although statistically significant discharge-related reductions in two of the water properties were observed during the January 2006 survey, the reductions were measured very close to a diffuser port, and well within the boundary of the ZID at Stations 4 (Figure 2). Receiving-water limitations do not apply to measurements within the ZID because the discharged wastewater is thought to be undergoing rapid initial mixing with the surrounding seawater. This was certainly the case for the large anomalies in salinity and density that were associated with Perturbation P1, which was located just above the seafloor near a diffuser port. The very low density associated with this perturbation was indicative of a highly buoyant plume that would undergo significant additional mixing as it rose through the water column.

Accordingly, the amplitudes of the shallower salinity anomalies at Stations 4 and 5 (Perturbations P2 and P3) were much smaller than those associated with the deep Perturbation P1. The smaller-amplitude salinity anomalies indicate that buoyancy-induced mixing had increased dilution by more than five-fold relative to the dilution measured within the turbulent jet. Accordingly, the two shallow perturbations were associated with only slight anomalies in temperature, transmissivity, DO, and pH. Clearly, these shallow anomalies were not caused by the presence of wastewater constituents. Otherwise, anomalies in these properties would also have been apparent at much higher amplitudes in the measurements of wastewater that were recorded shortly after ejection in Perturbation P1. Instead, the shallow anomalies in these water properties were generated by the upward displacement of deep ambient seawater that was entrained by the rising effluent plume. This is an important consideration because seawater limitations promulgated in the COP restrict attention to changes caused by the presence of waste materials.

Outfall Performance

The large salinity anomaly measured in the turbulent ejection jet close to a diffuser port demonstrated that the receiving-water objectives of the COP were being met at depth, well within the ZID. These high-precision observations demonstrated that the turbulent jet was achieving dilutions approaching the minimum critical dilution of 133:1 specified in the NPDES permit. Thus, the dilution objective was nearly achieved without consideration of the substantial additional dilution provided by the buoyant plume's subsequent rise through the water column. With the added buoyancy-induced mixing, measured dilutions increased five fold, to at least 669:1. These high-precision observations demonstrated that the diffuser structure was operating better than predicted by modeling, and that the discharged wastewater experienced high levels of dilution well within the ZID. With the higher dilution ratio (669:1) that was determined from actual measurements during the January 2006 survey, contaminant concentrations within the wastewater could have been more than quadruple the limits specified in the NPDES discharge permit, and the receiving-water objectives of the California Ocean Plan (COP) would still have been achieved.

NPDES Permit Limits

The seawater properties measured during the January 2006 survey were statistically evaluated for compliance with the pertinent receiving-water limitations promulgated by the NPDES discharge permit and the COP. Specifically, the permit and COP state that the discharge shall not cause

1. *natural light to be significantly reduced at any point outside the initial dilution zone as the result of the discharge of waste;*
2. *the dissolved oxygen concentration outside the zone of initial dilution to fall below 5.0 mg/L or to be depressed more than 10 percent from that which occurs naturally;*
3. *the pH outside the zone of initial dilution to be depressed below 7.0, raised above 8.3, or changed more than 0.2 units from that which occurs naturally; or*

4. *temperature of the receiving water to adversely affect beneficial uses.*

The COP (SWRCB 1997) further defines a ‘*significant*’ difference as ‘*...a statistically significant difference in the means of two distributions of sampling results at the 95 percent confidence level.*’ For each observation in Tables B-1 through B-6, the statistical significance of departures from mean conditions at a given depth level were determined with an analysis of variance that compares a single observation with the mean of a larger set of samples (Sokal and Rohlf 1997, p228; Ury 1976). Although 15 independent hypothesis tests were performed at each depth level, no Bonferroni adjustment to the error rate was included, so the tests are conservative. Specifically, Bonferroni adjustment indicates that the actual confidence level for the overall null hypothesis test for differences in properties is higher, around 99.7%, rather than the 95% level that applies to a single test. The standard deviation that was applied in the tests was determined from the entire data set to reflect the full range in ambient properties, including vertical variations.

Light Transmittance

Based on the statistical analysis, there were four stations where significant reductions in instrumentally recorded light transmittance were found beyond the ZID. As show in Table B-5, significant anomalies in the transmissivity field were found at Stations 1, 5, 11, 13. However, the transmissivity anomaly observed near the seafloor at Station 5 was associated with an increase in water clarity, not a reduction. Because the anomaly contained less turbid water, it could not have caused a “*...reduction in the transmittance of natural light...*” Moreover, all of the anomalies were located well below the 8-m euphotic zone where little natural light penetrates. Finally, none of the significant transmissivity anomalies were generated “*...as the result of the discharge of waste*” (SWRCB 1997). As discussed in the *Lateral Variability* section, the anomalies were an artifact of slight variation in the thickness of the bottom nepheloid layer (BNL). Other discharge-related transmissivity anomalies were also observed, but none were statistically significant. The turbidity anomalies in the upper water column associated with Perturbations P2 and P3 were generated by the movement of ambient seawater. Finally, not only was the turbidity anomaly associated with Perturbation P1 measured at a depth below the euphotic zone, but it was located well within the ZID, where receiving-water limitations do not apply.

Dissolved Oxygen

Although it is not explicitly stated in the NPDES discharge permit, the COP specifies that the DO limitation only applies to reductions that occur “*...as a result of the discharge of oxygen demanding waste materials.*” Clearly, then, the DO limitation does not apply to reductions in DO caused by the movement of ambient waters, regardless of whether or not they were induced by the physics of the discharge. Thus, the slightly reduced DO concentrations observed in the upper water column at Stations 4 and 5, which were generated by entrainment of ambient seawater, would not be subject to the limitations for that reason alone. However, the anomaly at Station 4 would also not be subject to the limitations because it was recorded well within the ZID. Even so, all of the statistically significant DO anomalies complied with the numerical limits specified in the permit. Specifically, none of the DO concentrations measured during the survey fell below the 5 mg/L minimum specified in the Basin Plan and the NPDES discharge permit (Table B-4). Similarly, the ambient DO concentrations within the deep water mass, were naturally depleted due to respiration and oxidation after a long period without replenishment from direct exchange with the atmosphere. These ambient DO concentrations at depth were lower than those of the discharge-related anomalies in the upper water column at Stations 4 and 5, so the anomalies would have to be considered too small “*...to be depressed more than 10 percent from that which occurs naturally.*”

pH

As with most of the anomalies in other seawater properties, the two discharge-related pH anomalies were not statistically significant, were generated by entrainment of ambient seawater and not the presence of wastewater constituents, and in the case of the Station-4 anomalies, were restricted to the ZID where the receiving-water limitations in the permit do not apply. Regardless of their applicability, all of the pH anomalies complied with the numerical limits specified in the permit. In fact, the range in pH among all of the measurements was only 0.083 pH units, so none of the measurements can be considered changed by ‘...more than 0.2 pH units from that which occurs naturally.’ The range across the entire pH field remained between 7.837 and 7.920, and thus all of the measurements also complied with the lower (7.0 pH) and upper (8.3 pH) bounds on discharge-induced pH changes.

Temperature and Salinity

The total range in temperature of 0.7°C across all observations was largely due to naturally occurring vertical stratification. Even if changes this large were generated by the discharge, they would be considered too small ‘...to adversely affect beneficial uses....’ The observed temperature range was much less than the large-scale spatial variability in sea-surface temperature shown in the satellite image on the cover of this report. The small, discharge-induced decreases in temperature (-0.27°C), which are visually apparent in the vertical sections at Stations 4 and 5, resulted from the upward displacement of naturally occurring, cooler bottom water, rather than as a result of warmer wastewater constituents.

Although salinity anomalies provide the best tracer of discharged effluent, their actual amplitude (0.276‰) was small compared to spatial differences in salinity that occur along the south-central California coast. In any regard, the observed range in both the measured temperature (0.7°C) and salinity (0.28‰) across all data collected during the January 2006 survey was too small to be considered harmful to marine biota or deleterious to beneficial uses.

Conclusions

All of the measurements recorded during the January 2006 survey complied with the receiving-water limitations specified in the NPDES discharge permit. The discharge-related anomalies that were found within the upper water column at Stations 4 and 5 were caused by the upward displacement of ambient seawater and not the presence of wastewater constituents. Salinity measurements recorded close to a diffuser port at Station 4 demonstrated that discharged wastewater was undergoing rapid mixing within the turbulent discharge jet. The dilution levels achieved by the momentum of the jet alone were close to those predicted by modeling for the entire dilution process. This confirmed that the diffuser structure and the outfall were operating better than would be expected from the modeling.

REFERENCES

- California Department of Fish and Game (CDFG). 2000. Black Rockfish, *Sebastes melanops*, 1993-1999 Commercial Catch by Ports & Blocks. In: Volume 1, Marine Fisheries Profiles. California Department of Fish and Game, Marine Region. December 2000.
- Davis, R.E., J.E. Dufour, G.J. Parks, and M.R. Perkins. 1982. Two Inexpensive Current-Following Drifters. Scripps Institution of Oceanography, University of California, San Diego, La Jolla, California. SIO Reference No. 82-28. December 1982.
- Fischer, H.B., E.J. List, R.C.Y. Koh, J. Imberger, and N.H. Brooks. 1979. Mixing in Inland and Coastal Waters. New York: Academic Press, 483 p.
- Kuehl, S.A., C.A. Nittrouer, M.A. Allison, L. Ercilio, C. Faria, D.A. Dukat, J.M. Jaeger, T.D. Pacioni, A.G. Figueiredo, and E.C. Underkoffler 1996. Sediment deposition, accumulation, and seabed dynamics in an energetic fine-grained coastal environment. *Continental Shelf Research*, 16: 787-816.
- Marine Research Specialists (MRS). 1998a. City of Morro Bay and Cayucos Sanitary District, Offshore Monitoring and Reporting Program, Water Column Sampling, March 1998 Survey. Prepared for the City of Morro Bay, CA. April 1998.
- Marine Research Specialists (MRS). 1998b. City of Morro Bay and Cayucos Sanitary District, Offshore Monitoring and Reporting Program, Semiannual Benthic Sampling Report, April 1998 Survey. Prepared for the City of Morro Bay, CA. July 1998.
- Marine Research Specialists (MRS). 1998c. City of Morro Bay and Cayucos Sanitary District, Offshore Monitoring and Reporting Program, Water Column Sampling, July 1998 Survey. Prepared for the City of Morro Bay, CA. August 1998.
- Marine Research Specialists (MRS). 2000. City of Morro Bay and Cayucos Sanitary District, Offshore Monitoring and Reporting Program, 1999 Annual Report. Prepared for the City of Morro Bay, California. February 2000.
- Marine Research Specialists (MRS). 2001. City of Morro Bay and Cayucos Sanitary District, Offshore Monitoring and Reporting Program, 2000 Annual Report. Prepared for the City of Morro Bay, California. February 2001.
- Marine Research Specialists (MRS). 2002. City of Morro Bay and Cayucos Sanitary District, Offshore Monitoring and Reporting Program, 2001 Annual Report. Prepared for the City of Morro Bay, California. February 2002.
- Marine Research Specialists (MRS). 2003. City of Morro Bay and Cayucos Sanitary District, Offshore Monitoring and Reporting Program, 2002 Annual Report. Prepared for the City of Morro Bay, California. February 2003.

- Marine Research Specialists (MRS). 2004. City of Morro Bay and Cayucos Sanitary District, Offshore Monitoring and Reporting Program, 2003 Annual Report. Prepared for the City of Morro Bay, California. February 2004.
- Marine Research Specialists (MRS). 2005. City of Morro Bay and Cayucos Sanitary District, Offshore Monitoring and Reporting Program, 2004 Annual Report. Prepared for the City of Morro Bay, California. February 2005.
- Marine Research Specialists (MRS). 2006. City of Morro Bay and Cayucos Sanitary District, Offshore Monitoring and Reporting Program, 2005 Annual Report. Prepared for the City of Morro Bay, California. February 2006.
- Morro Group, Inc. 2000. MFS Globenet Corp./WorldCom Network Services Fiber Optic Cable Project Final Environmental Impact Report. SCH No. 98091053. Volume I. Submitted to: County of San Luis Obispo Department of Planning and Building. Prepared in association with Arthur D. Little, Inc. and Marine Research Specialists. January 2000.
- Regional Water Quality Control Board (RWQCB) - Central Coast Region. 1994. Water Quality Control Plan (Basin Plan) Central Coast Region. Available from the RWQCB at 81 Higuera Street, Suite 200, San Luis Obispo, California. 148p. + Appendices.
- Regional Water Quality Control Board (RWQCB) - Central Coast Region. 1998. Administrative Extension of Waste Discharge Requirements/National Pollution Discharge Elimination System (NPDES) CA0047881, Order 92-67. Letter to Mr. William Boucher, Director of Public Works, City of Morro Bay from Roger W. Briggs, Executive Officer. 10 April 1998.
- Regional Water Quality Control Board (RWQCB) - Central Coast Region and the Environmental Protection Agency (EPA) – Region IX. 1998a. Waste Discharge Requirements (Order No. 98-15) and National Pollutant Discharge Elimination System (Permit No. CA0047881) for City of Morro bay and Cayucos Sanitary District, San Luis Obispo County. 11 December 1998.
- Regional Water Quality Control Board (RWQCB) - Central Coast Region and the Environmental Protection Agency (EPA) – Region IX. 1998b. Monitoring and Reporting Program No. 98-15 for City of Morro Bay and Cayucos Sanitary District, San Luis Obispo County. 11 December 1998.
- Sea-Bird Electronics, Inc. (SBE) 1989. Calculation of M and B Coefficients for the Sea-Tech Transmissometer. Application Note No. 7, Revised September 1989.
- Sea-Bird Electronics, Inc. (SBE) 1993. SBE 13/22/23/30 Dissolved Oxygen Sensor Calibration and Deployment. Application Note No. 13-1, rev B, Revised April 1993.
- Sokal, R.R. and F.J. Rohlf. 1997. Biometry: the Principals and Practice of Statistics in Biological Research, 3rd ed. New York: W.H. Freeman and Company, 850 p.
- Southern California Bight Pilot Project Field Coordination Team (SCBPPFCT). 1995. Field Operation Manual for Marine Water-Column, Benthic, and Trawl monitoring in Southern California. August 22, 1995.

State Water Resources Control Board (SWRCB). 1997. Water quality control plan, ocean waters of California, California Ocean Plan. California Environmental Protection Agency. Effective July 23, 1997.

Tetra Tech. 1992. Technical Review City of Morro Bay, CA Section 301(h) Application for Modification of Secondary Treatment Requirements for a Discharge into Marine Waters. Prepared for the U.S. Environmental Protection Agency, Region IX, San Francisco, CA by Tetra Tech, Inc., Lafayette, CA. February 1992.

Ury, H.K. 1976. A comparison of four procedures for multiple comparisons among means (pairwise contrasts) for arbitrary sample sizes. *Technometrics*, 18: 89–97.

APPENDIX A

Water Quality Profiles and Vertical Sections

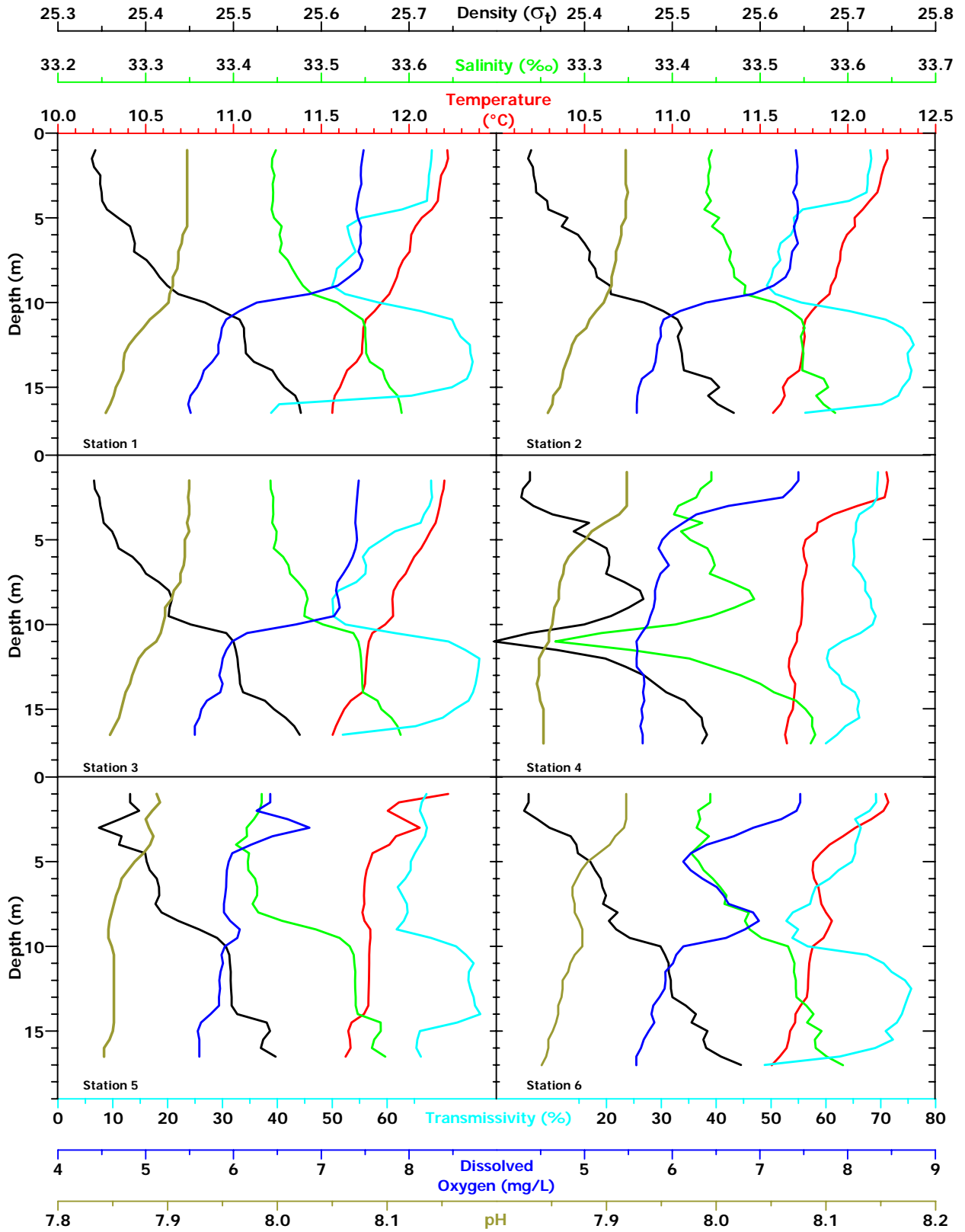


Figure A-1. Vertical Profiles of Water-Quality Parameters for Stations 1 through 6 measured on 17 January 2006

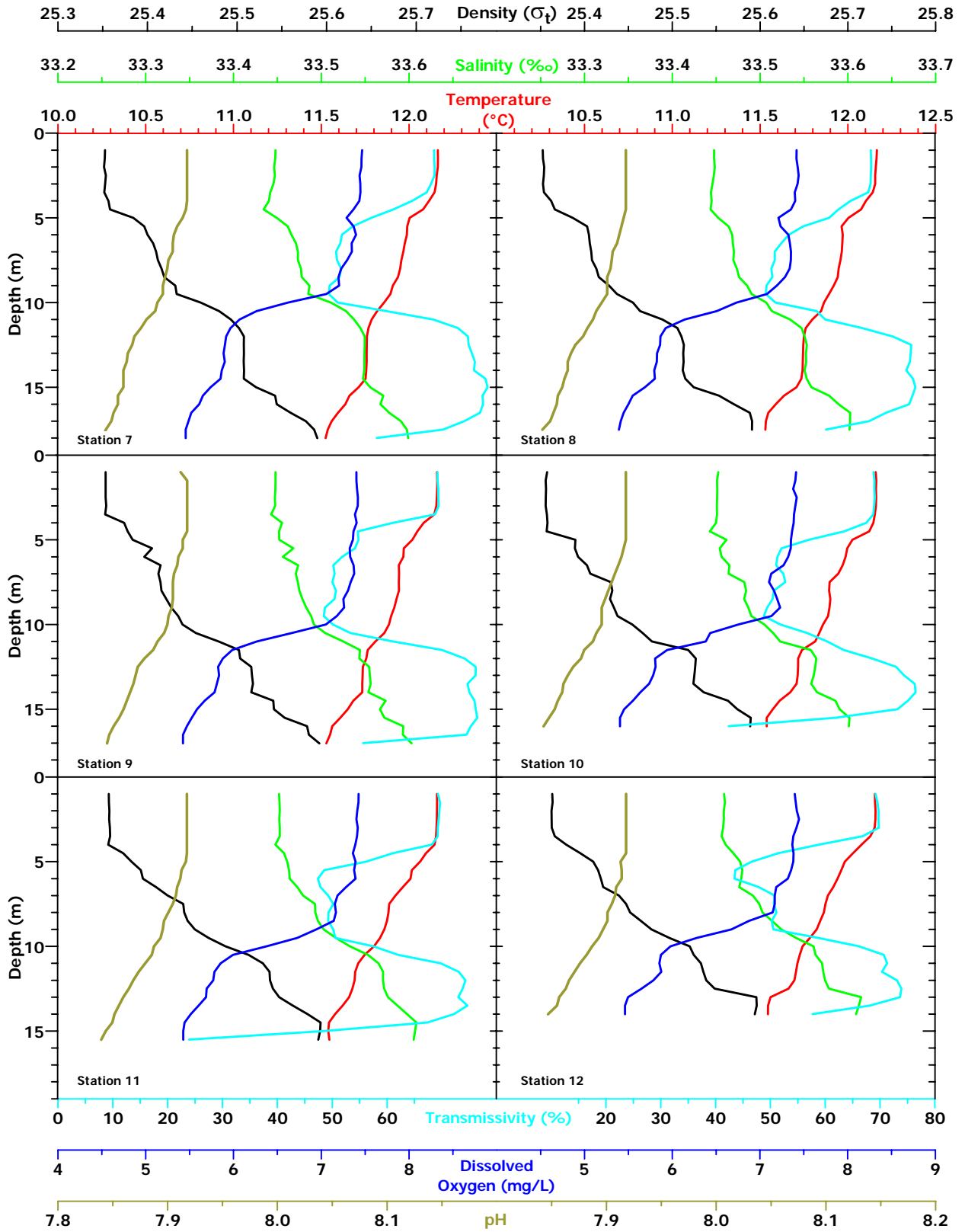


Figure A-2. Vertical Profiles of Water-Quality Parameters for Stations 7 through 12 measured on 17 January 2006

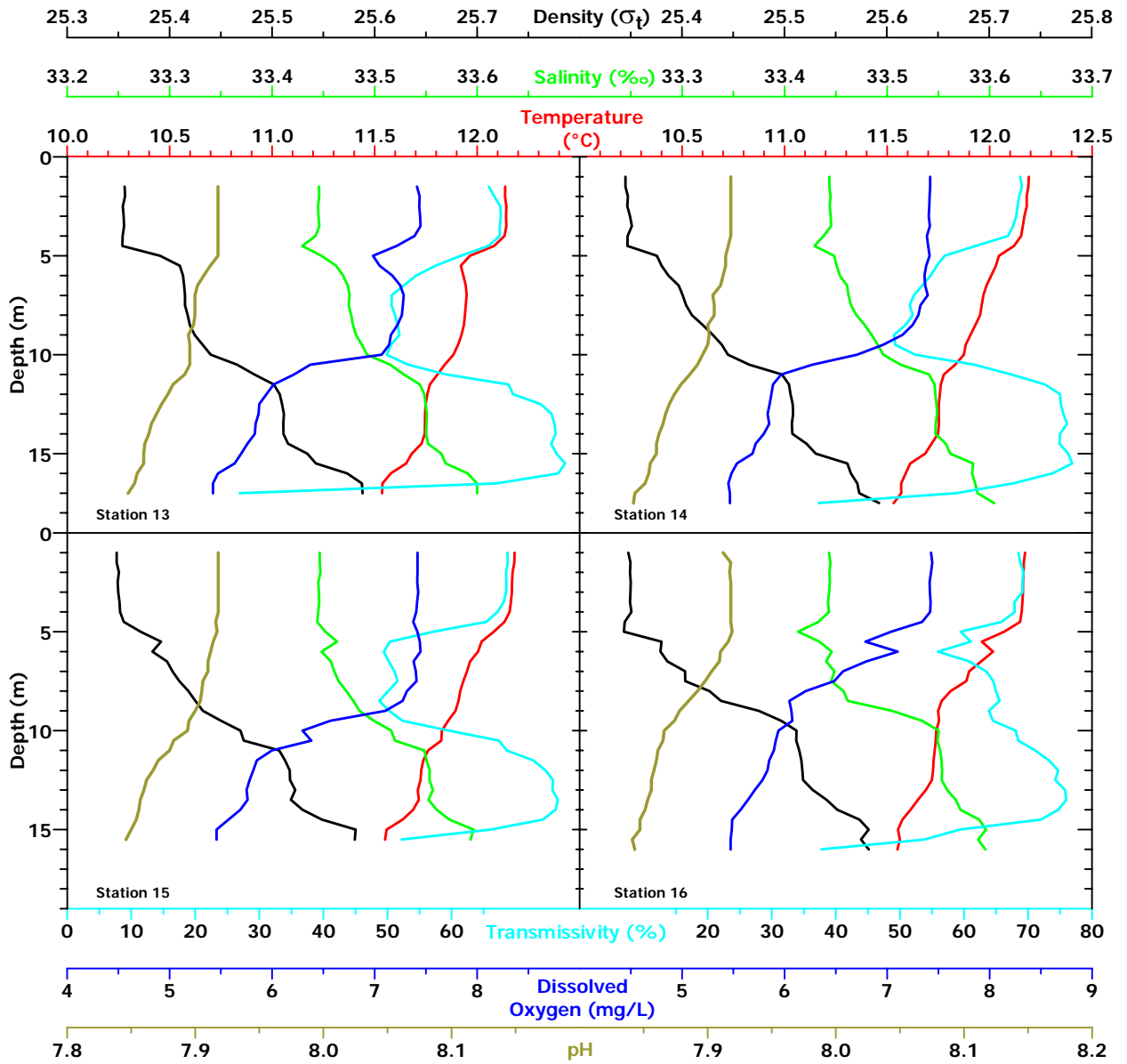


Figure A-3. Vertical Profiles of Water-Quality Parameters for Stations 13 through 16 measured on 17 January 2006

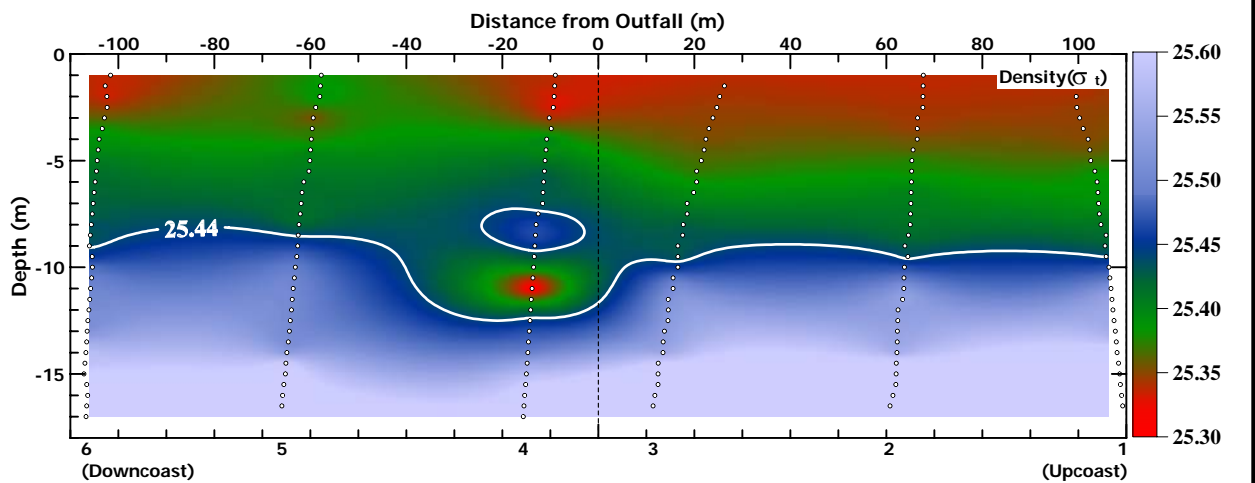
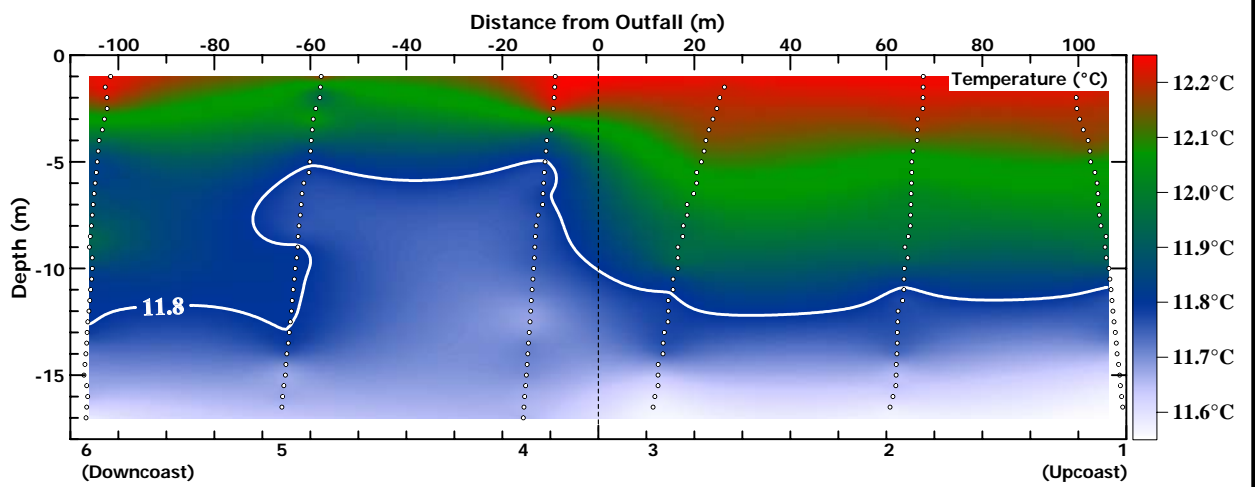
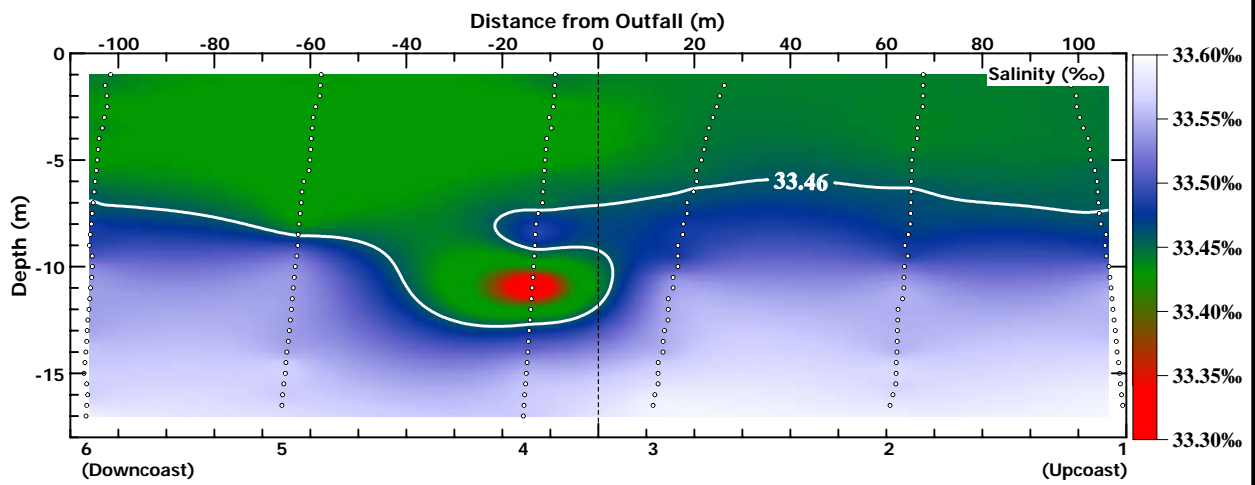


Figure A-4. Along-Shore Transects of Salinity, Temperature, and Density on 17 January 2006

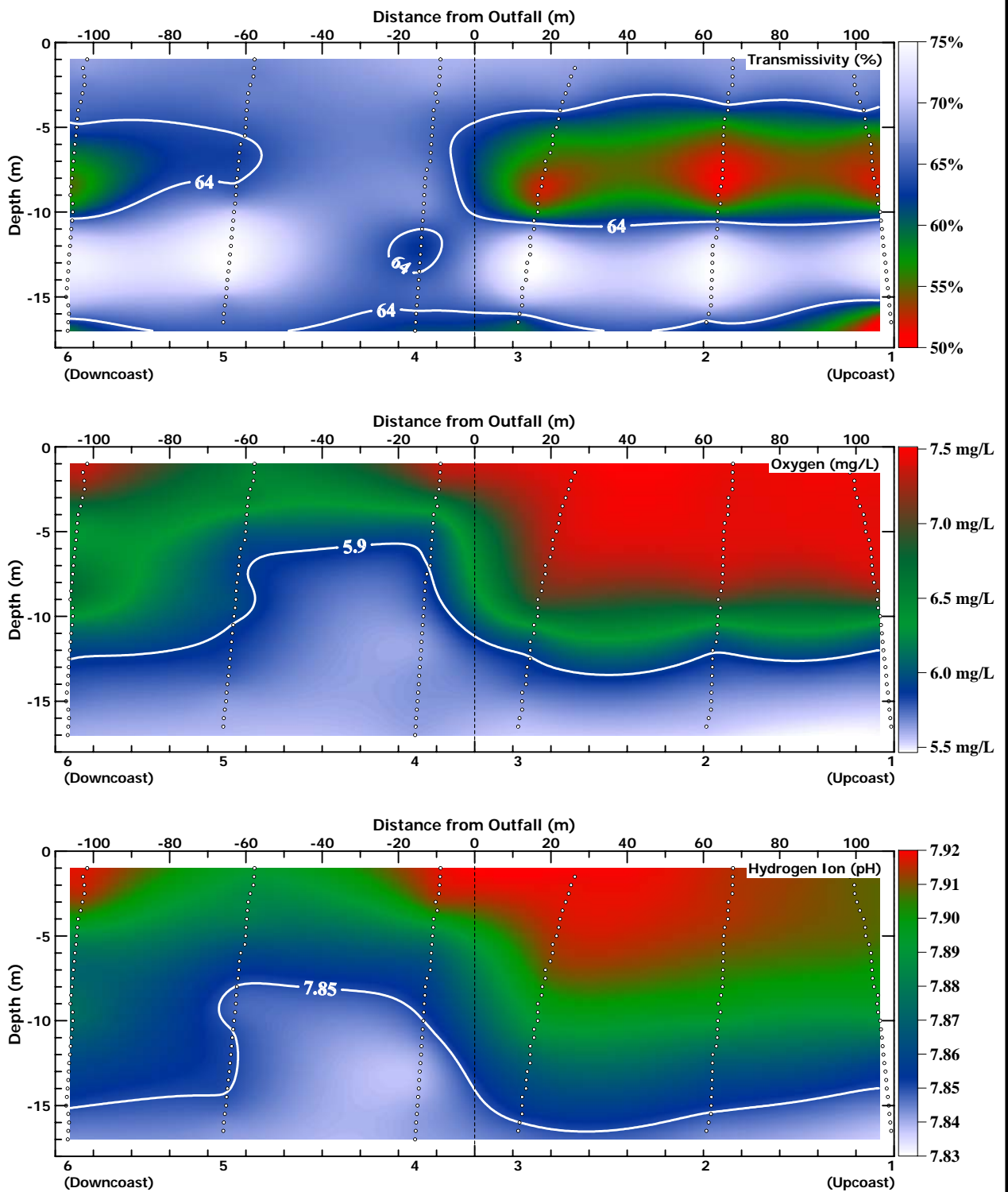


Figure A-5. Along-Shore Transects of Transmissivity, Oxygen, and pH on 17 January 2006

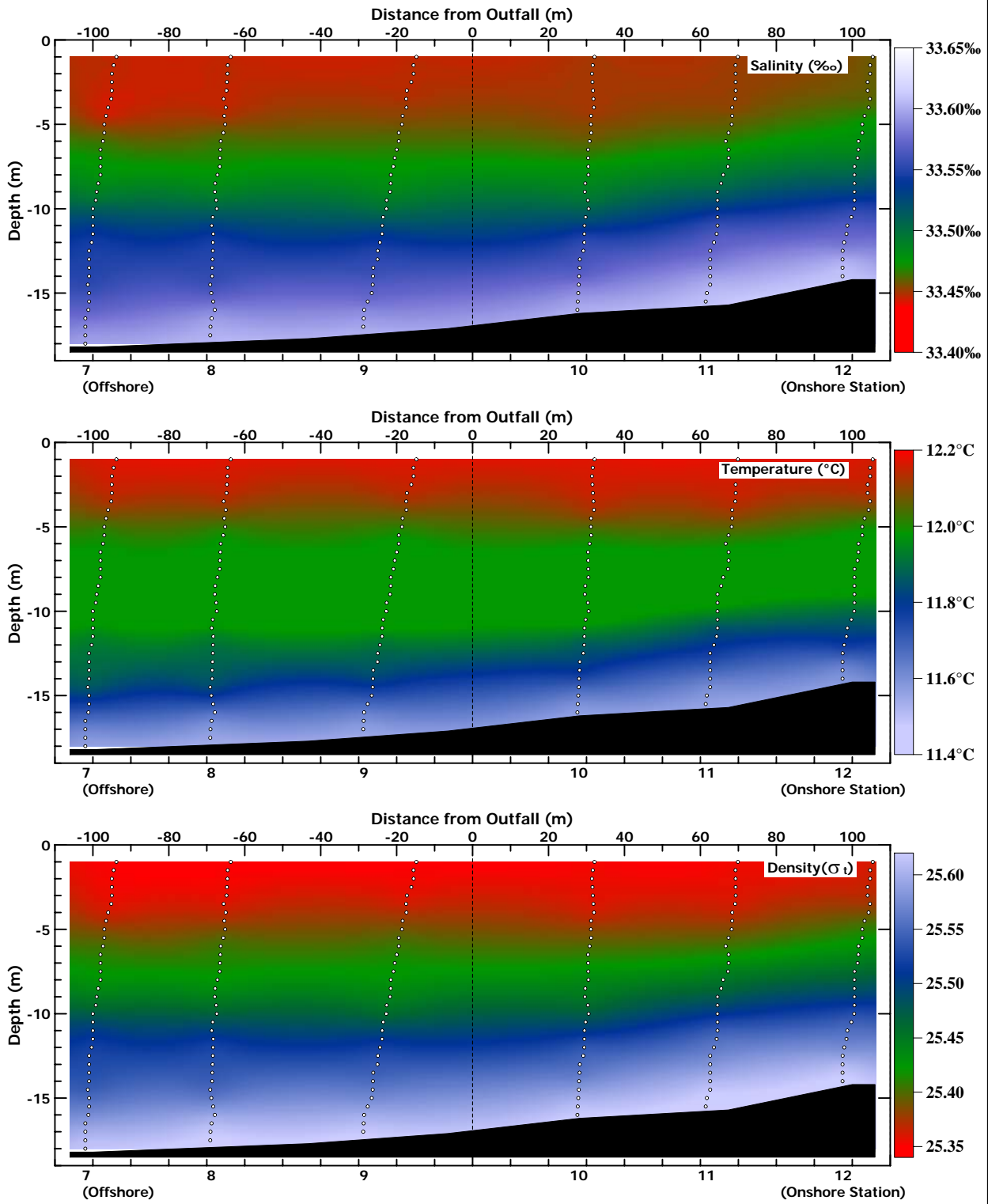


Figure A-6. Cross-Shore Transects of Salinity, Temperature, and Density on 17 January 2006

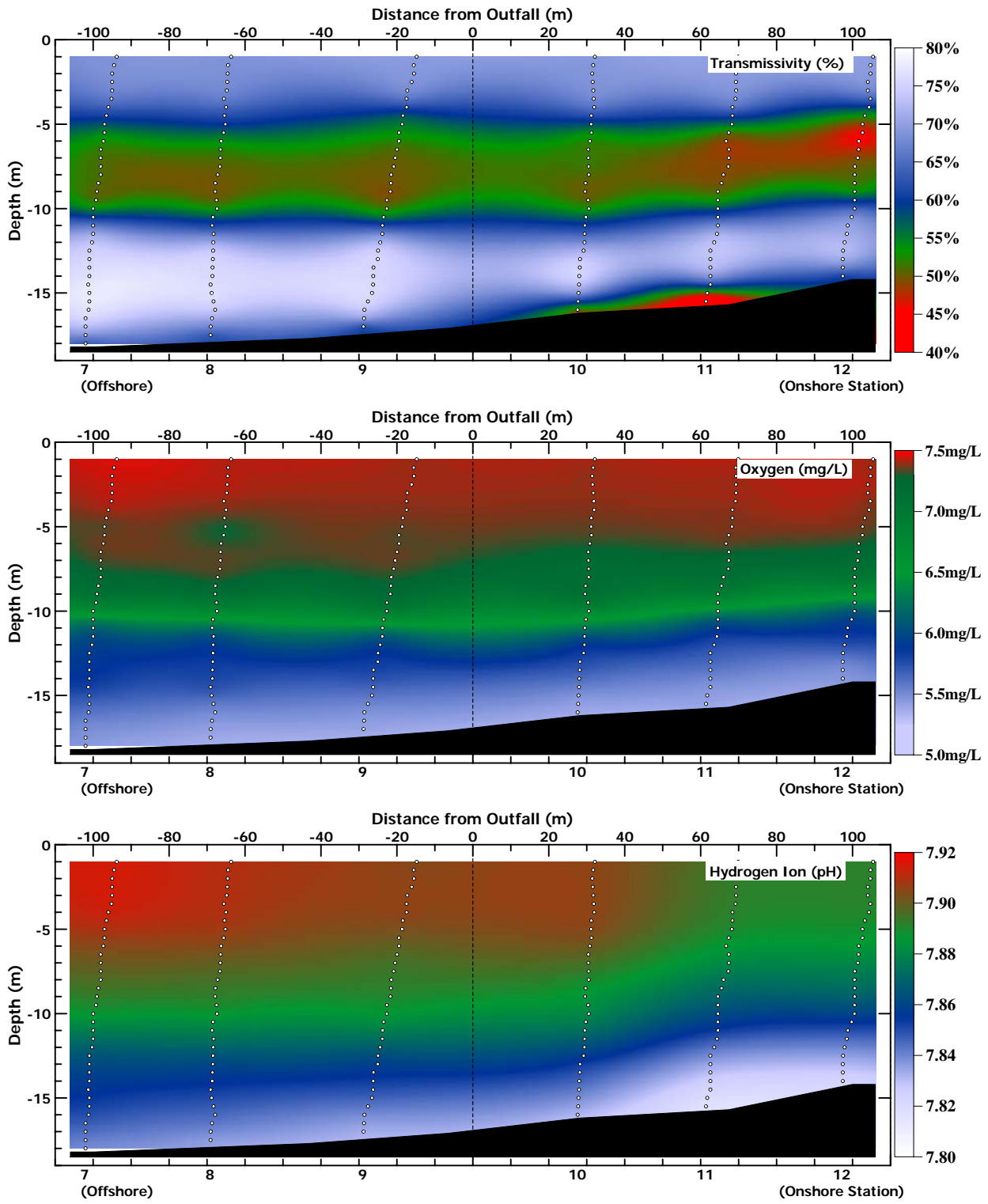


Figure A-7. Cross-Shore Transects of Transmissivity, Oxygen, and pH on 17 January 2006

APPENDIX B

Tables of Profile Data and Standard Observations

Table B-2. Salinity¹ on 17 January 2006

Depth (m)	Salinity (‰)															
	1	2	3	4	5	6	7	8	9	10	11	12	13	14	15	16
1.0	33.448	33.445		33.445	33.432	33.443	33.448	33.448	33.448	33.452	33.452	33.459		33.444	33.446	33.443
1.5	33.444	33.441	33.442	33.445	33.432	33.443	33.448	33.448	33.448	33.451	33.452	33.460	33.446	33.444	33.446	33.445
2.0	33.444	33.443	33.442	33.432	33.430	33.429	33.446	33.448	33.448	33.451	33.453	33.459	33.446	33.445	33.447	33.444
2.5	33.447	33.441	33.446	33.427	33.423	33.432	33.447	33.447	33.447	33.451	33.452	33.459	33.445	33.444	33.445	33.444
3.0	33.445	33.441	33.445	33.407	33.415	33.428	33.446	33.446	33.447	33.451	33.453	33.458	33.445	33.445	33.446	33.443
3.5	33.445	33.439	33.445	33.402	33.416	33.442	33.442	33.444	33.443	33.451	33.453	33.456	33.446	33.445	33.446	33.442
4.0	33.445	33.444	33.444	33.434	33.403	33.432	33.440	33.445	33.456	33.450	33.448	33.461	33.442	33.438	33.445	33.443
4.5	33.444	33.436	33.449	33.410	33.418	33.421	33.434	33.444	33.452	33.443	33.458	33.470	33.430	33.429	33.444	33.433
5.0	33.446	33.453	33.449	33.421	33.417	33.430	33.449	33.452	33.452	33.462	33.461	33.477	33.448	33.448	33.452	33.413
5.5	33.455	33.445	33.446	33.440	33.417	33.436	33.462	33.464	33.468	33.454	33.463	33.480	33.462	33.451	33.463	33.434
6.0	33.453	33.458	33.457	33.445	33.425	33.446	33.466	33.468	33.456	33.456	33.464	33.479	33.469	33.454	33.448	33.446
6.5	33.455	33.462	33.463	33.449	33.427	33.455	33.471	33.469	33.474	33.465	33.473	33.476	33.474	33.461	33.457	33.440
7.0	33.453	33.467	33.465	33.443	33.427	33.462	33.473	33.470	33.471	33.464	33.479	33.492	33.476	33.462	33.461	33.449
7.5	33.462	33.465	33.474	33.466	33.422	33.459	33.473	33.470	33.473	33.482	33.493	33.499	33.475	33.465	33.465	33.445
8.0	33.467	33.470	33.482	33.488	33.428	33.487	33.477	33.474	33.475	33.484	33.493	33.503	33.477	33.470	33.472	33.457
8.5	33.473	33.471	33.485	33.493	33.456	33.483	33.478	33.476	33.479	33.482	33.496	33.514	33.479	33.478	33.479	33.462
9.0	33.479	33.483	33.482	33.471	33.494	33.488	33.487	33.485	33.483	33.487	33.503	33.524	33.482	33.485	33.485	33.505
9.5	33.490	33.482	33.481	33.444	33.521	33.502	33.485	33.490	33.489	33.490	33.517	33.541	33.488	33.491	33.499	33.534
10.0	33.518	33.517	33.502	33.404	33.532	33.532	33.511	33.507	33.492	33.505	33.533	33.561	33.493	33.496	33.516	33.550
10.5	33.533	33.535	33.537	33.319	33.537	33.536	33.528	33.513	33.505	33.515	33.553	33.563	33.515	33.513	33.520	33.549
11.0	33.547	33.547	33.542	33.267	33.538	33.539	33.537	33.534	33.525	33.523	33.565	33.571	33.529	33.541	33.549	33.552
11.5	33.550	33.551	33.544	33.353	33.539	33.539	33.545	33.547	33.544	33.558	33.571	33.572	33.544	33.546	33.551	33.553
12.0	33.550	33.546	33.545	33.420	33.539	33.541	33.550	33.551	33.543	33.564	33.570	33.574	33.549	33.547	33.554	33.554
12.5	33.551	33.548	33.546	33.448	33.539	33.541	33.550	33.553	33.555	33.563	33.572	33.578	33.550	33.548	33.554	33.553
13.0	33.551	33.549	33.547	33.478	33.539	33.541	33.549	33.552	33.555	33.561	33.576	33.615	33.551	33.549	33.557	33.559
13.5	33.556	33.549	33.547	33.500	33.539	33.553	33.549	33.553	33.556	33.558	33.587	33.613	33.551	33.547	33.553	33.567
14.0	33.570	33.548	33.548	33.516	33.542	33.561	33.549	33.551	33.554	33.565	33.598	33.609	33.550	33.547	33.561	33.572
14.5	33.573	33.572	33.564	33.541	33.568	33.554	33.548	33.553	33.573	33.586	33.608		33.552	33.557	33.573	33.590
15.0	33.578	33.578	33.569	33.552	33.568	33.570	33.556	33.559	33.567	33.591	33.607		33.565	33.562	33.597	33.596
15.5	33.587	33.564	33.580	33.560	33.560	33.562	33.571	33.579	33.572	33.602	33.605		33.569	33.584	33.594	33.589
16.0	33.590	33.572	33.587	33.559	33.558	33.563	33.567	33.590	33.593	33.601			33.591	33.583		33.596
16.5	33.592	33.585	33.591	33.563	33.573	33.576	33.577	33.603	33.593				33.600	33.586		
17.0				33.558		33.594	33.591	33.603	33.603				33.600	33.588		
17.5							33.598	33.602						33.604		
18.0							33.599									

¹ Values enclosed in boxes were significantly lower than the mean of other salinity measurements at the same distance above the seafloor.

Table B-3. Seawater Density¹ on 17 January 2006

Depth (m)	Density (sigma-t)															
	1	2	3	4	5	6	7	8	9	10	11	12	13	14	15	16
1.0	25.343	25.339		25.338	25.382	25.336	25.353	25.352	25.353	25.357	25.357	25.363		25.345	25.348	25.348
1.5	25.339	25.336	25.341	25.338	25.382	25.336	25.352	25.353	25.353	25.356	25.357	25.364	25.356	25.345	25.348	25.350
2.0	25.341	25.341	25.342	25.330	25.393	25.331	25.352	25.354	25.353	25.356	25.357	25.362	25.357	25.347	25.351	25.349
2.5	25.348	25.342	25.347	25.328	25.371	25.346	25.354	25.354	25.353	25.356	25.357	25.362	25.354	25.347	25.349	25.350
3.0	25.348	25.344	25.348	25.342	25.347	25.360	25.353	25.353	25.354	25.356	25.358	25.363	25.355	25.349	25.350	25.350
3.5	25.350	25.345	25.351	25.364	25.373	25.384	25.352	25.354	25.353	25.357	25.358	25.366	25.355	25.351	25.351	25.349
4.0	25.351	25.357	25.352	25.405	25.370	25.391	25.356	25.362	25.374	25.358	25.356	25.379	25.354	25.347	25.352	25.351
4.5	25.356	25.359	25.362	25.388	25.399	25.392	25.358	25.366	25.378	25.357	25.373	25.395	25.354	25.347	25.355	25.344
5.0	25.369	25.381	25.366	25.407	25.401	25.407	25.384	25.386	25.383	25.390	25.382	25.410	25.391	25.376	25.372	25.343
5.5	25.382	25.374	25.369	25.425	25.405	25.412	25.396	25.403	25.405	25.389	25.393	25.416	25.410	25.380	25.392	25.380
6.0	25.385	25.393	25.385	25.428	25.413	25.418	25.400	25.405	25.396	25.393	25.395	25.419	25.413	25.387	25.383	25.379
6.5	25.388	25.400	25.394	25.428	25.415	25.420	25.406	25.406	25.415	25.403	25.410	25.421	25.414	25.397	25.398	25.386
7.0	25.387	25.406	25.400	25.425	25.416	25.425	25.410	25.408	25.412	25.407	25.423	25.439	25.415	25.401	25.403	25.403
7.5	25.401	25.405	25.415	25.446	25.411	25.421	25.412	25.409	25.414	25.430	25.440	25.447	25.415	25.404	25.410	25.403
8.0	25.409	25.412	25.427	25.463	25.418	25.438	25.416	25.413	25.416	25.432	25.441	25.452	25.418	25.410	25.418	25.427
8.5	25.416	25.414	25.430	25.467	25.437	25.428	25.419	25.416	25.421	25.429	25.445	25.464	25.420	25.420	25.425	25.438
9.0	25.425	25.429	25.427	25.450	25.461	25.436	25.431	25.428	25.427	25.433	25.453	25.476	25.424	25.430	25.433	25.475
9.5	25.437	25.430	25.426	25.430	25.482	25.451	25.433	25.437	25.434	25.438	25.468	25.497	25.432	25.439	25.450	25.497
10.0	25.468	25.468	25.451	25.399	25.491	25.486	25.459	25.455	25.439	25.455	25.487	25.520	25.440	25.445	25.469	25.512
10.5	25.487	25.490	25.492	25.338	25.495	25.492	25.480	25.463	25.454	25.466	25.513	25.525	25.466	25.466	25.472	25.512
11.0	25.507	25.506	25.500	25.297	25.496	25.496	25.493	25.489	25.480	25.477	25.529	25.533	25.483	25.498	25.507	25.515
11.5	25.512	25.511	25.503	25.369	25.497	25.496	25.502	25.506	25.502	25.518	25.54	25.536	25.502	25.505	25.513	25.517
12.0	25.512	25.506	25.505	25.424	25.497	25.498	25.508	25.510	25.504	25.527	25.537	25.539	25.507	25.506	25.517	25.518
12.5	25.514	25.509	25.505	25.447	25.497	25.498	25.508	25.513	25.516	25.526	25.540	25.548	25.510	25.508	25.517	25.518
13.0	25.514	25.511	25.507	25.468	25.498	25.500	25.508	25.513	25.517	25.525	25.547	25.596	25.512	25.509	25.523	25.528
13.5	25.523	25.512	25.507	25.480	25.498	25.516	25.507	25.513	25.518	25.524	25.562	25.596	25.511	25.507	25.518	25.541
14.0	25.544	25.513	25.511	25.493	25.504	25.527	25.508	25.512	25.516	25.536	25.579	25.594	25.511	25.508	25.530	25.552
14.5	25.550	25.544	25.536	25.514	25.538	25.522	25.508	25.515	25.541	25.563	25.593		25.515	25.522	25.549	25.573
15.0	25.558	25.553	25.546	25.523	25.542	25.540	25.521	25.525	25.541	25.574	25.593		25.534	25.531	25.581	25.582
15.5	25.570	25.541	25.559	25.533	25.534	25.535	25.542	25.553	25.553	25.589	25.591		25.543	25.562	25.581	25.575
16.0	25.575	25.552	25.569	25.535	25.531	25.539	25.544	25.570	25.578	25.589			25.573	25.565		25.582
16.5	25.577	25.570	25.576	25.540	25.548	25.556	25.560	25.588	25.580				25.588	25.571		
17.0				25.534		25.578	25.577	25.591	25.592				25.588	25.573		
17.5							25.586	25.591						25.592		
18.0							25.590									

¹ Values enclosed in boxes were significantly lower than the mean of other density measurements at the same distance above the seafloor.

Table B-5. Light Transmittance¹ across a 0.25-m path on 17 January 2006

Depth (m)	Light Transmittance (%)															
	1	2	3	4	5	6	7	8	9	10	11	12	13	14	15	16
1.0	68.17	68.10		69.49	67.17	69.11	68.59	68.31	69.19	68.79	69.29	69.17		68.79	68.72	68.47
1.5	68.08	68.26	68.04	69.41	66.32	69.15	68.59	68.36	69.20	68.97	69.66	69.53	65.82	69.05	68.80	68.80
2.0	67.89	68.05	68.05	69.32	65.97	67.96	68.68	68.36	69.33	68.95	69.54	69.73	66.66	68.61	68.52	69.25
2.5	67.62	67.62	68.22	69.37	66.68	65.31	68.63	68.32	69.35	69.03	69.43	69.69	67.64	68.35	68.56	69.10
3.0	67.57	67.61	67.71	68.44	67.29	66.34	68.01	68.26	69.41	68.90	69.25	69.79	67.69	68.13	68.53	69.10
3.5	67.36	67.41	66.75	66.07	66.92	65.90	67.22	67.84	68.73	68.74	69.23	66.80	67.54	67.66	68.14	67.86
4.0	67.30	64.21	66.10	65.50	66.01	65.36	64.56	64.60	61.09	67.50	68.17	58.85	67.52	66.85	67.18	67.90
4.5	62.76	55.79	61.45	65.47	65.06	65.33	61.15	62.41	54.67	63.44	61.03	51.44	65.77	61.76	65.43	65.86
5.0	55.31	54.15	59.10	64.97	64.33	64.76	57.13	60.69	54.77	57.01	56.23	46.60	61.43	56.97	57.16	59.47
5.5	52.75	54.36	56.73	65.09	64.30	62.33	53.72	55.97	54.15	52.01	48.55	43.60	57.50	55.74	50.38	61.05
6.0	53.11	53.60	55.57	65.19	63.32	60.65	51.77	53.36	51.82	51.27	47.40	43.44	54.50	54.81	49.43	55.92
6.5	53.60	51.71	56.17	64.90	61.96	58.10	51.47	51.97	50.19	51.03	47.84	47.89	52.53	53.48	50.18	60.83
7.0	54.24	51.29	56.07	66.34	62.78	57.53	50.71	50.80	50.43	52.34	49.25	50.74	50.67	52.18	51.10	63.44
7.5	52.60	51.69	54.37	67.18	63.61	57.12	50.89	50.78	50.03	52.71	50.20	50.62	50.62	51.50	51.55	64.56
8.0	50.85	50.40	51.16	67.16	63.73	53.96	51.63	50.19	50.67	50.59	49.31	51.11	51.19	52.00	50.11	64.96
8.5	50.53	50.06	50.07	68.17	63.04	52.79	51.31	50.34	50.42	50.40	49.25	50.22	51.59	50.85	48.74	65.55
9.0	50.01	49.23	50.14	68.29	61.74	54.93	49.52	49.27	48.67	49.39	50.20	50.54	51.88	49.08	50.25	63.86
9.5	52.35	50.78	50.24	69.08	68.03	53.87	49.39	49.16	48.47	48.78	50.58	58.75	50.57	49.24	52.36	64.53
10.0	58.49	55.52	52.44	68.51	72.60	56.67	51.03	50.91	50.12	51.81	57.54	66.17	49.88	52.37	59.59	68.06
10.5	66.14	64.29	61.39	66.30	74.38	67.52	59.89	58.45	53.34	56.71	62.02	70.68	53.20	61.62	67.40	68.45
11.0	71.85	70.87	71.19	62.93	75.78	70.51	68.39	59.99	61.11	60.33	69.76	71.29	59.22	67.38	68.60	71.09
11.5	72.52	73.97	74.27	60.56	74.92	71.94	72.90	66.71	70.03	63.39	73.07	70.34	68.91	72.64	72.76	73.23
12.0	73.38	75.32	76.82	60.20	74.82	74.43	74.76	72.31	74.14	68.58	74.28	73.08	69.60	74.99	74.66	74.69
12.5	75.09	76.01	76.68	60.67	75.21	75.55	74.89	75.68	76.17	72.91	73.79	73.88	73.92	75.11	75.85	74.25
13.0	75.20	74.87	76.43	62.38	75.79	74.93	75.48	75.58	76.15	74.36	72.99	73.64	75.63	75.48	75.76	75.76
13.5	75.61	75.06	76.12	62.95	76.04	74.37	76.00	75.43	74.67	76.33	74.64	68.14	76.04	76.09	76.58	75.96
14.0	75.25	75.60	75.68	65.28	77.00	73.84	75.85	74.78	75.03	76.49	72.19	57.70	76.23	74.98	76.24	74.73
14.5	74.56	75.24	74.85	66.06	72.77	72.93	77.95	76.00	75.96	75.08	67.33		75.54	74.89	74.27	72.00
15.0	71.82	73.98	72.32	65.74	65.97	70.89	78.31	76.45	76.15	73.18	48.48		76.37	76.26	66.14	59.36
15.5	64.42	73.18	70.14	66.08	65.51	72.22	77.41	75.92	76.45	61.84	23.92		77.72	76.89	52.23	53.85
16.0	40.32	70.16	65.20	63.56	65.34	68.98	77.49	75.32	75.28	42.42			76.66	73.77		37.76
16.5	38.90	56.26	51.96	62.02	66.15	62.50	76.93	71.08	74.49				67.10	67.65		
17.0				60.01		48.86	74.08	67.98	55.66				26.98	58.73		
17.5							70.21	60.17						37.33		
18.0							58.15									

¹ Values enclosed in boxes were significantly different from the mean of other transmissivity measurements at the same distance above the seafloor.

Table B-6. Detrended¹ pH on 17 January 2006

Depth (m)	Hydrogen Ion Concentration (pH)															
	1	2	3	4	5	6	7	8	9	10	11	12	13	14	15	16
1.0	7.918	7.918		7.919	7.890	7.918	7.918	7.918	7.912	7.918	7.918	7.918		7.918	7.918	7.912
1.5	7.918	7.918	7.920	7.919	7.893	7.918	7.918	7.918	7.918	7.918	7.918	7.918	7.918	7.918	7.918	7.918
2.0	7.918	7.918	7.920	7.919	7.886	7.918	7.918	7.918	7.918	7.918	7.918	7.918	7.918	7.918	7.918	7.917
2.5	7.918	7.918	7.919	7.919	7.880	7.918	7.918	7.918	7.918	7.918	7.918	7.918	7.918	7.918	7.918	7.918
3.0	7.918	7.918	7.920	7.919	7.883	7.916	7.918	7.918	7.918	7.918	7.918	7.918	7.918	7.918	7.918	7.918
3.5	7.918	7.920	7.920	7.912	7.887	7.908	7.918	7.918	7.918	7.918	7.918	7.918	7.918	7.918	7.918	7.918
4.0	7.918	7.918	7.918	7.899	7.884	7.903	7.918	7.918	7.918	7.918	7.918	7.918	7.918	7.918	7.918	7.918
4.5	7.918	7.918	7.920	7.887	7.878	7.893	7.917	7.918	7.918	7.918	7.918	7.918	7.918	7.916	7.916	7.918
5.0	7.918	7.918	7.916	7.881	7.870	7.883	7.914	7.916	7.914	7.918	7.917	7.913	7.918	7.914	7.917	7.919
5.5	7.918	7.914	7.916	7.873	7.864	7.877	7.909	7.914	7.914	7.916	7.913	7.914	7.912	7.914	7.914	7.916
6.0	7.914	7.914	7.916	7.866	7.858	7.873	7.906	7.912	7.910	7.914	7.912	7.914	7.907	7.912	7.912	7.910
6.5	7.913	7.912	7.915	7.862	7.856	7.869	7.905	7.910	7.909	7.911	7.909	7.909	7.902	7.910	7.910	7.909
7.0	7.910	7.909	7.912	7.861	7.853	7.869	7.905	7.906	7.906	7.908	7.908	7.908	7.900	7.904	7.910	7.903
7.5	7.910	7.909	7.912	7.858	7.851	7.871	7.901	7.905	7.905	7.905	7.905	7.905	7.900	7.905	7.906	7.898
8.0	7.909	7.907	7.906	7.857	7.849	7.871	7.900	7.904	7.905	7.902	7.901	7.901	7.900	7.905	7.905	7.892
8.5	7.905	7.905	7.904	7.857	7.847	7.875	7.898	7.901	7.905	7.899	7.897	7.901	7.899	7.900	7.904	7.885
9.0	7.905	7.905	7.898	7.853	7.846	7.878	7.896	7.901	7.904	7.896	7.896	7.897	7.895	7.901	7.900	7.878
9.5	7.902	7.901	7.898	7.852	7.846	7.878	7.896	7.901	7.901	7.896	7.894	7.893	7.896	7.900	7.895	7.874
10.0	7.901	7.898	7.896	7.851	7.849	7.878	7.891	7.896	7.900	7.896	7.888	7.887	7.896	7.896	7.894	7.866
10.5	7.893	7.891	7.894	7.848	7.851	7.871	7.889	7.891	7.897	7.891	7.886	7.882	7.896	7.892	7.883	7.865
11.0	7.884	7.885	7.890	7.848	7.851	7.867	7.881	7.888	7.891	7.888	7.880	7.876	7.892	7.886	7.880	7.861
11.5	7.878	7.882	7.880	7.843	7.851	7.865	7.876	7.883	7.887	7.880	7.874	7.871	7.883	7.879	7.871	7.860
12.0	7.871	7.873	7.874	7.839	7.851	7.860	7.870	7.879	7.879	7.877	7.869	7.866	7.879	7.874	7.867	7.858
12.5	7.865	7.869	7.871	7.839	7.851	7.860	7.868	7.872	7.873	7.870	7.865	7.863	7.874	7.870	7.862	7.856
13.0	7.861	7.867	7.868	7.839	7.851	7.859	7.864	7.868	7.871	7.865	7.860	7.857	7.870	7.867	7.860	7.856
13.5	7.860	7.864	7.866	7.837	7.851	7.856	7.863	7.865	7.869	7.861	7.856	7.855	7.866	7.865	7.857	7.853
14.0	7.860	7.861	7.862	7.839	7.851	7.856	7.860	7.865	7.866	7.860	7.852	7.847	7.864	7.862	7.856	7.851
14.5	7.857	7.860	7.860	7.840	7.851	7.854	7.860	7.862	7.863	7.856	7.850		7.861	7.860	7.854	7.847
15.0	7.853	7.858	7.858	7.843	7.850	7.851	7.860	7.860	7.860	7.853	7.844		7.860	7.860	7.850	7.847
15.5	7.851	7.852	7.856	7.843	7.847	7.847	7.855	7.856	7.856	7.848	7.840		7.860	7.855	7.846	7.841
16.0	7.848	7.851	7.852	7.843	7.842	7.847	7.855	7.855	7.851	7.843			7.855	7.854		7.843
16.5	7.844	7.847	7.848	7.843	7.842	7.845	7.851	7.852	7.847				7.853	7.851		
17.0				7.843		7.841	7.849	7.849	7.845				7.848	7.843		
17.5							7.844	7.842						7.842		
18.0							7.841									

¹ Measured pH levels were corrected for temporal drift to account for ongoing equilibration of the pH sensor.

Table B-8. Ancillary Observations on 17 January 2006 during the Receiving-Water Survey

Station	Location		Diffuser Distance (m)	Time (PST)	Air Temperature (°C)	Cloud Cover (%)	Wind Avg (kt)	Wind Max (kt)	Wind Dir (from) (°T)	Swell Ht/Dir (ft/°T)	Secchi Depth (m)
	Latitude	Longitude									
1	35° 23.257' N	120° 52.503' W	107.5	09:45:21	16.9	10	1.0	1.9	SE	1-2 /W	4.0
2	35° 23.230' N	120° 52.504' W	57.5	09:49:15	14.8	10	1.3	2.6	SE	1-2 /W	4.0
3	35° 23.206' N	120° 52.502' W	13.9	09:51:44	13.8	10	2.5	3.7	SE	1-2 /W	4.0
4	35° 23.190' N	120° 52.507' W	17.1	09:54:47	14.4	10	1.6	3.0	SE	1-2 /W	3.0
5	35° 23.164' N	120° 52.502' W	64.7	09:58:13	14.3	10	1.6	2.6	SE	1-2 /W	4.0
6	35° 23.144' N	120° 52.507' W	102.5	10:02:07	14.4	10	2.3	3.1	SE	1-2 /W	4.0
7	35° 23.197' N	120° 52.575' W	106.7	09:09:05	17.9	15	0.3	0.8	SE	1-2 /W	4.0
8	35° 23.197' N	120° 52.546' W	62.7	09:03:57	15.8	15	0.6	1.9	SE	1-2 /W	4.0
9	35° 23.198' N	120° 52.523' W	28.6	09:00:52	15.4	15	0.6	1.5	SE	1-2 /W	4.0
10	35° 23.199' N	120° 52.489' W	22.5	08:57:13	13.8	15	2.4	3.4	SE	1-2 /W	4.0
11	35° 23.197' N	120° 52.467' W	56.6	08:54:23	15.8	15	1.0	2.0	SE	1-2 /W	4.0
12	35° 23.195' N	120° 52.448' W	85.7	08:52:12	14.4	20	3.3	4.0	SE	1-2 /W	4.0
13	35° 23.172' N	120° 52.528' W	61.2	09:13:56	16.1	10	0.5	1.0	SE	1-2 /W	4.0
14	35° 23.223' N	120° 52.532' W	60.8	09:28:46	15.8	10	0.9	1.5	SE	1-2 /W	4.0
15	35° 23.223' N	120° 52.480' W	67.6	09:23:29	16.4	10	1.1	1.8	SE	1-2 /W	4.0
16	35° 23.167' N	120° 52.472' W	67.2	09:17:25	15.0	10	0.7	1.1	SE	1-2 /W	4.0

There was no visual expression of the effluent plume at the sea surface. Neither odors nor debris of sewage origin were observed at any time during the survey. Neither odors nor debris of sewage origin were observed at any time during the survey.

Tidal Conditions (Pacific Standard Time)

High Tide: 00:21 3.62 ft
 Low Tide: 05:05 2.13 ft
 High Tide: 11:06 5.06 ft
 Low Tide: 18:14 -0.08 ft